COCHLEATA controls spatial regulation of cytokinin and auxin during nodule development

Karen Velandia[1], Muhammad Nouman Sohail[1ϕ], Tiana Scott[1], Alejandro Correa-Lozano[1], Alannah Mannix[1] and Eloise Foo[1*]

[1] Discipline of Biological Sciences, School of Natural Sciences, University of Tasmania, Private Bag 55, Hobart, Tasmania, 7001, Australia

[ϕ]Current address- Elizabeth Macarthur Agricultural Institute, New South Wales Department of Primary Industries and Regional Development, Menangle, Sydney, NSW 2568, Australia.

[*]Author for correspondence: Eloise Foo

Email: Eloise.foo@utas.edu.au

Running title: *COCHLEATA* shapes hormone dynamics in nodules

Abstract

Root nodules develop in some legumes that host nitrogen-fixing bacteria and likely evolved through modifications of the ancestral lateral root program with plant hormones playing key regulatory roles. Members of the NOOT-BOP-COCH-LIKE transcriptional co-regulator family suppress root identity in legume nodules, including *Pisum sativum coch1* that display root-nodule hybrids. However, how COCH/NOOT interacts with hormones to control nodule organogenesis is unclear. We show that *PsCOCH* (*COCHLEATA*) is required for spatial tight regulation of auxin and cytokinin during nodule organogenesis and identify key hormone and signalling genes regulated by *COCH*. COCH suppresses cytokinin levels and response during nodule formation, as cytokinin levels are elevated in *Pscoch* abnormal nodules and this is mirrored by ectopic cytokinin-responsive *TCSn::GUS* expression in *Pscoch* nodule apices, nodule vasculature and in root-like tissue. In contrast, *PsCOCH* promotes auxin accumulation and precise auxin response patterning in nodules, as *Pscoch* mutants show significantly reduced auxin levels and severely altered auxin-responsive DR5::GUS expression patterns. RNAseq analysis revealed that *Pscoch* developing nodules have gene expression profiles more similar to root primordia, with increased expression of defence and auxin response genes (IAA and ARF) and reduced expression of cytokinin biosynthesis genes (*IPT3, CYP735A* and *LOG2)* compared to wild type. We found gibberellin is unlikely to act downstream of *PsCOCH*, as *Pscoch* and gibberellin-deficient double mutants still form root-nodule hybrids. Ectopic constitutive expression of *PsCOCH* also produces root-nodule hybrids and we found intriguing links between autoregulation of nodulation pathway and *COCH*, suggesting that a complex feedback mechanism acts in *COCH* control of nodule identity.

Key words: Autoregulation of nodulation; auxin; COCHLEATA; cytokinin; gibberellin; nodulation; root development.

Introduction

The formation of root nodules that host nitrogen-fixing bacteria in selected plants of the Fabid clade offer a unique advantage to these plants in nitrogen-poor environments and are also a significant nitrogen input into natural and agricultural environments. Decades of research in legume-rhizobial symbioses has uncovered many of the genes and hormonal signals controlling the two stages of legume nodulation, infection in the epidermis and nodule organogenesis in the inner root (Figure S3; Luo et al., 2023; Roy et al., 2020; Velandia et al., 2022). The infection program shares evolutionary history with the more ancient and widespread arbuscular mycorrhizal symbiosis (Radhakrishnan et al., 2020), while nodule organogenesis has overlaps with lateral root program including the cell layers that these organs arise from, as well as overlapping transcriptional networks and hormone dynamics (Lee et al., 2024; Schiessl et al., 2019; Soyano et al., 2019).

Intriguing players in the cross over of the root and nodule programs are the orthologous members of the NOOT-BOP-COCH-LIKE (NBCL) gene family *COCHLEATA/COCH2* in *Pisum sativum L.* and *NOOT/NOOT2* in *Medicago truncatula*. Pea *coch* and *Medicago noot* mutants display root-nodule hybrids (Couzigou et al., 2012; Ferguson and Reid, 2005), and act somewhat redundantly with *coch2* and *noot2* respectively to maintain nodule identity (Liu et al., 2023). The determinate nodulator *Lotus japonicus* only contains one NBCL member, *NBCL1*, and at least some *Ljnbc1* mutants display root-nodule hybrids, suggesting a conserved role for this gene in nodule organogenesis (Liu et al., 2018; Magne et al., 2018a). Studies in *Medicago* have revealed that *NOOT* likely functions by establishing boundaries between different cell populations within nodules to ensure proper cell fate specification (Shen et al., 2020b). This boundary formation is crucial for separating the infected tissue, where nitrogen fixation occurs, from the root vasculature. In addition, in *noot* mutants, there is a shift in the gradient of mitotic activity; pericycle and endodermis-derived cells exhibit increased mitotic activity, while the mitotic activity of outer cortical cells is suppressed (Shen *et al.*, 2020b). This altered pattern of cell division contributes to the unique morphology observed in *Mtnoot* nodules that resemble that of actinorhizal nodules with central vascular tissue. *NOOT* also has a mild influence of the size of root apical meristem (RAM) in *Medicago*, with *noot* mutants displaying changes in spatial development of root cell files, although the overall impact on root architecture has not been reported (Shen et al., 2019). It is not clear if COCH/NOOT also influence the earlier stages on nodulation including rhizobial infection, as well as other key

elements of root development including root architecture or interaction with arbuscular mycorrhizal symbiosis.

Plant hormones including auxin, cytokinin and gibberellin are key regulators of cell division, differentiation and organ development, including regulating lateral root and nodule development (reviewed by Azarakhsh and Lebedeva, 2023; Jan et al., 2024; Velandia *et al.*, 2022). Indeed, hormones may be a key mechanism in the common and divergent developmental pathways in root and nodule development; auxin and gibberellin have positive roles in the development of both organs (Tu et al., 2024; Ubeda-Tomás et al., 2009; Velandia et al., 2024), while cytokinin promotes the development of nodules but suppresses lateral root emergence and growth (e.g. Casimiro et al., 2001; Gonzalez-Rizzo et al., 2006; Riefler et al., 2006). However, relatively little is known about how NOOT/COCH interacts with plant hormones to control nodule development. In *Medicago*, there is disruption in pattern of gibberellin (as monitored by the biosensor GIBBERELLIN PERCEPTION SENSOR 2) in root-nodule hybrids of *noot1 noot2* double mutants, in particular a reduction of gibberellin in the nodule meristem (Drapek et al., 2024). As outlined below, transcript profiling in the days following inoculation with rhizobia indicate auxin and cytokinin pathway gene expression are disrupted in *noot noot2* mutant and *NOOT/NOOT2* overexpression lines compared to wild type (Lee *et al.*, 2024).

Detailed mutant and RNAseq analysis have indicated some of the factors that may interact with *NOOT/NOOT2* to control nodule identity in *Medicago*. *NOOT/NOOT2* appears to act downstream of transcription factors *LSH1/LHS2* belonging to the LIGHT-SENSITIVE SHORT HYPOCOTYL (LSH) family that are key factors mediating the divergence of lateral roots and nodules in *Medicago* (Lee *et al.*, 2024). An interaction between these pathways is supported by the fact that there is strong overlap in the genes mis-regulated in *noot noot2* and *lsh1 lsh2* double mutant roots, and *lsh1 lsh2* mutant displays at least some root-nodule hybrid structures (Lee *et al.*, 2024). However, the fact that ectopic expression of *NOOT/NOOT2* could not fully rescue *lsh1 lsh2* phenotype (Lee *et al.*, 2024) indicates these genes may also act in somewhat parallel roles during early nodule development. A range of auxin and cytokinin biosynthesis, transport and response proteins presented altered expression in *noot noot2* mutant and *NOOT/NOOT2* overexpression lines in the days following inoculation compared to wild type (Lee *et al.*, 2024). Indeed, the pattern of hormone gene expression in *noot noot2* was similar to that of *lsh1 lsh2* mutants, leading to the hypothesis that LSH acts via NOOT to regulate hormone dynamics (Lee *et al.*, 2024). An examination of auxin and cytokinin levels and

110 response during nodule organogenesis, accompanied by tissue specific RNAseq studies, would
111 enable us to identify nodule-specific targets acting downstream of NOOT/COCH.

112 Autoregulation of nodulation (AON) is a root-shoot-root systemic signalling system that limits
113 nodule number. AON signalling is enhanced by the presence of more mature nodules (Kassaw
114 et al., 2015; Li et al., 2009) and AON suppresses subsequent infection and nodule
115 organogenesis (reviewed by Roy and Muller, 2022; Yoro et al., 2019). Furthermore, studies in
116 at least in some legumes have revealed elements of the AON system (CLAVATA1, KLV,
117 miR2111) not only influence nodule number, but also independently influence the number of
118 lateral roots and lateral root development (Day et al., 1986; Goh et al., 2018; Lagunas et al.,
119 2019; Wopereis et al., 2000; Zhang et al., 2021), although this did not appear to be the case in
120 pea (Wang et al., 2020).Thus, it would be interesting to examine if root-nodule hybrids of
121 *coch/noot* mutants interact with the AON system in a similar way to wild type and if elements
122 of AON may influence the development of root-nodule hybrids in *coch*.

123 In this study, the interaction between *PsCOCH* and plant hormones auxin, cytokinin and
124 gibberellin in nodule development was examined in detail. This included examination of auxin
125 and cytokinin response using hormone-responsive promoter::*GUS* studies, hormone
126 measurements and tissue specific RNAseq in wild type and *coch* mutants. We found that
127 *PsCOCH* is required for spatial tight regulation of auxin and cytokinin during nodule
128 organogenesis and identify key hormone and signalling genes regulated by *COCH* during
129 nodule development. We also found that *PsCOCH* in the root appears to act specifically in
130 nodule organogenesis, with no obvious effect on rhizobial infection, root architecture or
131 consistent effect on colonisation by arbuscular mycorrhizal fungi.

132

133 **Results**

134 ***PsCOCH* impacts on nodulation, root development and arbuscular mycorrhizal**
135 **symbioses**

136 As the impact of *coch*/*noot*/*nbc1* mutations on infection thread development or arbuscular
137 mycorrhizal symbioses has not been reported in any species this was characterised in *coch-*
138 *JI2165, coch-JI2757* and corresponding wild type lines. Mutation of the *PsCOCH* gene did not
139 result in any change in number of infection threads (Figure 1A) and no consistent effect of
140 *coch-JI2165* mutation on infection thread number was observed across multiple independent
141 experiments (data not shown). *coch-JI2165* mutant lines developed a range of mature

142 nodulation phenotypes, including approximately 50% relatively normal nodules and
143 approximately 50% abnormal nodule types not seen in wild type lines (Figure 1B), including
144 nodules bearing root-like structures at tips (Figure 1C) and heart-shaped nodules with central
145 vascular system (with a clear invagination at nodule centre; Figure 1D to 1E), consistent with
146 other pea *coch* lines (Ferguson and Reid, 2005; Liu *et al.*, 2023). Sections taken through
147 nodules revealed that abnormal *coch-JI2165* nodules have reduced number of vascular bundles
148 (3 instead of 4 presents in single lobed WT nodules) and these strands are thickened (Figure
149 1D and 1F). The abnormal *coch* nodules have additional uninfected cell layers in the outer
150 cortex and the intermediate and nitrogen fixation zones of *coch* abnormal nodules contain less
151 rhizobia than wild type nodules (Figure 1D and 1E), indicating defects in bacterial colonization
152 and symbiosome formation.

153 Overall, the *coch-JI2165* mutation did not have a consistent effect on the number of developing
154 or mature nodules (Figure 1B; data not shown). There was also no consistent effect of *coch*
155 mutations on root architecture in plants grown under sterile conditions (Table S1), consistent
156 with previous reports of other *coch* alleles (Ferguson and Reid, 2005). We examined the
157 influence of two *coch* mutant alleles on arbuscular mycorrhizal symbiosis. A small but
158 significant increase in the amount of the root colonised by arbuscular mycorrhizal fungi,
159 including all fungal structures and arbuscules, was observed in *coch-JI2165* plants compared
160 to respective wild type plants, although no change was observed in colonisation rates in *coch-*
161 *JI2757* lines (Figure S1).

162 The regulation of nodule number is under strict control of the systemic autoregulation of
163 nodulation (AON) pathway (reviewed by Roy and Muller, 2022) and in pea this negative
164 feedback loop is activated by nodule primordia development (Li *et al.*, 2009). To explore if the
165 formation of abnormal *coch* nodules is regulated by the AON pathway, the phenotypes of
166 double mutants disrupted in COCH and key elements of the AON pathway, CLE peptide
167 receptors *Ps*NARK (CLV1 orthologue) and *Ps*CLV2, were examined (Figure 2). As previously
168 reported, *Psnark* and *Psclv2* single mutants display significant increase in nodule number (e.g.
169 Sagan and Duc, 1996), and a large increase in total nodule number was also observed in *Psnark*
170 *coch* and *Psclv2 coch* double mutants compared to wild type lines (Figure 2A). The *coch*
171 mutation did not have a consistent influence on total nodule number in different AON mutant
172 backgrounds. However, the proportion of abnormal nodules was actually enhanced in both
173 *Psnark coch* and *Psclv2 coch* compared to *coch* single mutant plants, rising from approximately
174 70% abnormal nodules in *coch* mutants to approximately 85-95% abnormal nodules in AON

175 mutant backgrounds. Several genes involved in the AON pathway showed differential
176 expression in *coch* mutant nodules (Figure S2D). The expression of the putative CLE receptor
177 genes *KLV1* and *KLV2* were upregulated in *coch* developing nodules, whereas their expression
178 remained unchanged in wild-type nodules compared to root primordia expression. In contrast,
179 the expression of *TML2*, a transcription factor that may act downstream of AON pathway to
180 suppresses nodulation (Gautrat et al., 2019; Lebedeva et al., 2022; Nishida et al., 2016),
181 increased in wild-type mature nodules but remained unchanged in *coch* mature nodule tissue,
182 suggesting that AON pathway activation may be at least partially dependent on *COCH*
183 function.

184

185 **RNAseq analysis of roots and nodules in wild type and *Pscoch* mutants**

186 Previous RNA-seq in *Medicago* investigated early expression profiles in *noot1/noot2* (within
187 72 h post inoculation; Lee *et al.*, 2024) but given *coch* largely acts during nodule organogenesis,
188 we performed tissue specific RNA-seq analysis on root primordia, developing nodules, and
189 mature nodules of wild-type and *coch*. Root primordia expression profiles were largely similar
190 between genotypes, with only 23 differentially expressed genes (DEGs) identified, and the
191 samples clustered closely in the principal component analysis (PCA) (Figure 3A). However,
192 developing *coch* nodules a more root-like transcript profile, clustering more closely with wild-
193 type root primordia than with wild-type developing nodules (Figure 3A). Indeed, *coch*
194 developing nodules showed roughly half as many differentially expressed genes as wild-type
195 developing nodules. (Figure 3A), indicating a divergence in expression profile in early nodule
196 development between *coch* and wild type. The transcript profile of mature nodules of wild-
197 type and *coch* overlapped and were distinct from developing nodules, suggesting the gene
198 expression patterns in mature nodules converge in the two genotypes.

199 To gain insight into the biological processes affected by the *coch* mutation, we performed Gene
200 Ontology (GO) enrichment analysis on the subset of genes that were differentially expressed
201 in wild-type developing and/or mature nodules but not differentially expressed in *coch* mutant
202 developing or mature nodules, relative to wild-type root primordia (Figure S2A-B). Genes
203 uniquely upregulated in wild-type nodules were enriched with GO terms predominantly
204 associated with energy and carbon metabolism, including key components of the tricarboxylic
205 acid (TCA) cycle and carbohydrate-derived energy production (Figure S2A). Other enriched
206 GO categories included lipid metabolism pathways, such as sphingolipid, isoprenoid, and

ubiquinone biosynthesis; pathways important for formation of the symbiosome, (Moore et al., 2021) and mitochondrial oxidative energy metabolism to sustain nitrogen fixation (Sin et al., 2024) respectively. Conversely, genes uniquely downregulated in wild-type nodules were enriched for GO terms related to plant defence, immune responses, and reactive oxygen species signalling (Figure S2B). This group included multiple leucine-rich repeat (LRR) resistance genes involved in effector triggered immunity (ETI) (Tong et al., 2023), and peroxidases. ETI responses are thought to be repressed during nodule development with some LRR proteins contributing to host specificity (Gourion et al., 2015; Yang et al., 2010). This suggests a role for COCH in suppressing defence responses to facilitate symbiosis. Notably, two genes putatively involved in root cap formation and stem cell differentiation in the root meristem also appeared to be downregulated in a *COCH*-dependent manner.

To investigate the genes potentially mis-regulated in *coch* that may contribute to the formation of chimeric nodule–root structures, we investigated the expression of genes previously characterized as regulators of root organogenesis (Figure S2C). Several genes that were differentially expressed in wild-type developing and mature nodules compared to wild type root primordia showed no significant changes in the corresponding *coch* mutant tissues. Notably, components of the auxin signalling pathway, including *ARF6/8* and the auxin influx transporter *AUX1*, were downregulated during nodule development in the wild type but remained unchanged in *coch* developing nodules and more closely resembled that of root primordia (Figure S2C). In addition, several key root development transcription factors (TFs) were differentially expressed in wild-type nodules but not in the *coch* mutant. Specifically, *coch* mutants showed reduced expression of *PLETHORA3* (*PLT3*) in developing nodules and *PLT5* in mature nodules compared to the corresponding wild-type tissues. PLT are known to orchestrate lateral root growth and differentiation of the emerging root layers (Du and Scheres, 2017; Santuari et al., 2016). Other important TFs involved in root and nodule development failed to be down-regulated in *coch* nodules (Figure S2C), including *HB2*, *GRF6* and members of the *KNOX* family (Dean et al., 2004; He et al., 2020; Qi and Zheng, 2013; Rodriguez et al., 2015; Yan et al., 2024). Conversely, LOB DOMAIN CONTAINING PROTEIN *LBD11*expression was reduced in *coch* mature nodules. LBD11, a homologue of *Arabidopsis thaliana* LBD3, functions in secondary root growth downstream of cytokinin signalling (Ye et al., 2021) and its accumulation has been shown to inhibit lateral root formation (Zuo et al., 2023). Other genes showing differential expression between wild-type and *coch* nodules were

239 associated with cell cycle regulation, cell wall modification, and epigenetic control (Figure
240 S2C).

241 Genes related to early symbiotic signalling, rhizobial infection, nodule organogenesis, and
242 nodule function displayed a delayed transcriptional response in *coch* developing nodules
243 (Figure S2D). These genes were mis-regulated in developing *coch* nodules but appeared to
244 recover to expression levels similar to wild type in mature nodules, suggesting a temporal delay
245 in the activation of the nodulation program in the *coch* plants. The expression of *COCH1* and
246 *COCH2* was not significantly different between wild-type and *coch* mutant nodules, indicating
247 that *COCH2* is not under feedback control by *COCH1*. Expression patterns of genes related to
248 auxin, cytokinin, and gibberellin signalling are discussed below.

249 **Constitutive overexpression of *PsCOCH* can induce root-nodule hybrids**

250 The effect of the loss of function of COCH/NOOT1/NBC1 is well understood across several
251 species but the impact of ectopic expression of COCH on nodulation is unknown. The full
252 length *PsCOCH* gene was expressed under both tissue-specific and constitutive promoter in
253 wilt type pea hairy roots (Figure 4). In pea roots, the *35S* promoter is constitutively expressed
254 in all root tissue, *AtCO2* promoter is expressed in basal meristematic zone as seen in
255 *Aarbidopsis* (Figure S3; Heidstra et al., 2004) and the *AtCASP* promoter is expressed in
256 endodermis (Velandia *et al.*, 2024). *CASP::GUS* was used as a control. Quantitative real-time
257 PCR analysis of whole root samples confirmed that *PsCOCH* expression was significantly
258 elevated in *35S::COCH* roots compared to *CASP::GUS* controls, while modest increases were
259 also observed in *CASP::COCH* and *CO2::COCH* roots (Figure S4).

260 Expression of *PsCOCH* under *CO2* promoter or *CASP* promoter had no observable effect on
261 nodule number or development compared to the *CASP::GUS* control (Figure 4A). Strikingly,
262 *35S::COCH* overexpression resulted the production of abnormal nodules exhibiting
263 characteristics similar to those of *coch* mutants. These included nodules with irregular shapes
264 (Figure 4C), thickened vascular strands, a reduced number of vascular strands (Figure 4D), and
265 root-nodule hybrids (Figure 4B). No changes in root architecture or vascular patterning were
266 observed in any of the constructs (data not shown).

267 **Elevated cytokinin levels and ectopic cytokinin response in *Pscoch* nodules**

268 Cytokinin is essential for nodule organogenesis; nodules develop at the site of cytokinin foci
269 that form due to tight spatial regulation of cytokinin biosynthesis and catabolism (reviwed by
270 Nadzieja et al., 2019; Velandia *et al.*, 2022). This positive role for cytokinin in nodule

organogenesis is contrasted with a negative role in lateral root development (Azarakhsh and Lebedeva, 2023; Laplaze et al., 2007; Reid et al., 2017). It has been proposed that this specific role for cytokinin in nodule organogenesis may be due to the key nodulation gene *NIN* upregulating cytokinin production that in turn promotes auxin biosynthesis via LBD16, STY and YUC to activate nodule organogenesis (Schiessl *et al.*, 2019).

We monitored endogenous cytokinin levels in mature nodules of wild type and *coch* mutant. The level of cytokinin trans-zeatin riboside (t-ZR) was significantly higher in *coch* mature nodules than levels found in mature wild type nodules (Figure 5A). Cytokinin response was also assessed using the *TCSn::GUS* reporter. In wild-type roots, *TCSn::GUS* activity was typically observed in cells surrounding infection threads connected to nodules and in most developing nodule primordia, as observed previously in pea (Figure 5B) (Velandia *et al.*, 2024). In wild type mature nodules *TCSn::GUS* signal is largely confined to the nodule meristem and has a faint presence in the vasculature (Figure 5F, 5I). Quantification of GUS presence indicated that 60–70% of wild-type infection threads, developing primordia, and mature nodules exhibited a detectable *TCSn::GUS* signal (Figure 5B). A different pattern of cytokinin response was observed in *coch* mutants. A significantly lower proportion of infection threads in *coch* mutants (approximately 20%) were associated with *TCSn::GUS* activity, while 100% of *coch* developing nodule primordia showed *TCSn::GUS* signal, significantly higher than observed in wild type lines (Figure 5B). Approximately 80-90% of *coch* nodules displayed *TCSn::GUS* signal, which was not significantly different to wild type (Figure 5B). However, ectopic or expanded cytokinin signalling were apparent in abnormal *coch* nodules including *TCSn::GUS* signal in thickened peripheral and central vascular strands and strong *TCSn::GUS* in the tips of heart shaped nodules and root-like structures subtending these abnormal nodules (Figure 5E-K). *TCSn::GUS* was expressed in the root tips of both wild type and *coch* mutants in a similar pattern (Figure 5L-M).

We analysed the expression of genes involved in cytokinin biosynthesis, catabolism, and signalling in the RNA-seq dataset. The developing nodules of *coch* plants exhibited an expression profile for cytokinin biosynthesis genes *IPT3*, *LOG2*, and *CYP735A10* that is more similar to root primordia, unlike the high expression in these genes observed in developing wild type nodules (Figure 3C). In addition, several type-A and type-B cytokinin response regulators also showed altered expression in *coch* developing and mature nodules (Figure 3C), indicating that cytokinin signalling is altered in the *coch* mutant background.

303 **Auxin levels in *Pscoch* mutant nodules are low and the pattern of auxin response is**
304 **severely altered compared to wild type**

305 The formation of auxin maxima at the site of nodule organogenesis is achieved through precise
306 regulation of auxin transport and/or auxin biosynthesis (reviewed by Velandia *et al.*, 2022).
307 Indeed, key cross over points in lateral root and nodule development programs involves the
308 activation of LBD16 that in turn promotes auxin biosynthesis genes *STY* and/or *YUC* (Schiessl
309 *et al.*, 2019; Shrestha et al., 2021; Soyano *et al.*, 2019). Auxin accumulation appears to occur
310 downstream of CK dependent activation of NIN and flavonoid synthesis (Ng et al., 2015;
311 Schiessl *et al.*, 2019; Suzaki et al., 2012). Given that cytokinin levels are elevated and cytokinin
312 response is mis-regulated in nodules of *coch* mutant plants (Figure 5), we investigated if this
313 might lead to abnormal auxin gene expression, auxin biosynthesis and/or auxin response
314 patterning in *coch* nodules (Figure 6).

315 Overall, the auxin response gene expression profile in *coch* developing nodules was up-
316 regulated compared to wild type developing nodules and more closely resembled that found in
317 root primordia (Figure 3C). In contrast to wild type nodules, in *coch* developing nodules a large
318 number of *IAA* genes—encoding auxin response repressors—failed to be downregulated.
319 Similarly, the expression of four *ARF* (Auxin Response Factor) genes in *coch* developing
320 nodules was the same as seen in root primordia, in contrast to the low expression in wild type
321 (Figure 3B). Auxin content (measured via LC-MS) and auxin response patterns (monitored
322 using the *DR5::GUS* reporter) were assessed in nodules and lateral roots of both *coch* mutant
323 and wild type plants (Figure 6). Auxin levels in root tips and developing nodules were
324 comparable between *coch* and wild type, but mature *coch* nodules contained significantly lower
325 auxin levels than mature wild type nodules (Figure 6A). Wild type and *coch* mutants expressed
326 *DR5::GUS* throughout the developing nodule primordia and also in young root vasculature,
327 lateral root primordia and root tips (Figure 6 B-F, Velandia *et al.*, 2024). As wild type nodules
328 developed, *DR5::GUS* expression became restricted to the nodule vasculature and nodule
329 meristem (Figure 6 I, L, O). However, as the *coch* nodules matured two distinct patterns of
330 *DR5::GUS* were observed. In *coch* nodules with root-like growths from tip, *DR5::GUS* signal
331 was only found in root-like tissues, including vascular tissue and meristem, with no *DR5::GUS*
332 signal in peripheral nodule vasculature or nodule meristem (Figure 6 K, N). Other patterns of
333 *DR5::GUS* staining were also observed in some maturing *coch* nodules; very strong auxin
334 response throughout the whole nodule that included cells containing bacteria (Figure 5H,

335 Figure S5) and in heart shaped mature *coch* nodules strong auxin response in the abnormal
336 central vascular tissue (Figure 5J, M).

337

338 ***PsCOCH* does not act via gibberellin to supress root identity in nodules**

339 In addition to key roles for auxin and cytokinin, gibberellin is a key promoter of nodule and
340 root development, while suppressing rhizobial infection (Ramon et al., 2021; Velandia *et al.*,
341 2024). Studies in pea suggest gibberellin acts upstream of cytokinin to suppress infection thread
342 progression and branching and also upstream of auxin in nodule primordia development
343 (Velandia *et al.*, 2024). Given the altered auxin and cytokinin response in of *coch* mutants
344 (Figures 2, 5 and 6), we examined the infection and nodulation phenotypes of *coch na* double
345 mutant plants compared to respective single mutant parents and wild-type line (Figure 7). These
346 plants carry disruptions in both *COCH* and *NA*, a gibberellin biosynthesis gene and these lines
347 have very low levels of active gibberellin.

348 As previously observed, gibberellin-deficient *na* mutants develop excessive number of
349 infection threads, including highly branched infection threads and develop very few nodules
350 that are underdeveloped (Figure 7A; McAdam et al., 2018; Velandia *et al.*, 2024). Interestingly,
351 double mutant *coch na* plants develop significantly less infection threads and branched
352 infection threads than *na* (Figure 7A). As outlined above, the excessive infection thread
353 development and branching in *na* mutants was correlated with overactivation of cytokinin
354 response (Velandia *et al.*, 2024). Gibberellin is important for nodule maturation, as both *na* and
355 *coch na* mutant plants develop very few mature nodules compared to wild type plants (Figure
356 7B). However, like observed in *coch* single mutants approximately 50% of mature nodules that
357 did form in *coch na* double mutants displayed characteristic abnormal phenotype, including
358 nodules with roots (Figure 7B, C). Therefore, gibberellin is not required for the development
359 of root-nodule hybrids and suggest gibberellin does not play a role in COCH control of nodule
360 development. We also examined the expression of genes involved in GA biosynthesis,
361 catabolism, and signalling in the RNA-seq dataset and found no consistent change in GA
362 biosynthetic or catabolic gene expression in the *coch* mutant tissue (Figure 3D). However,
363 some GA-responsive genes were expressed at lower levels in mature *coch* nodules than wild
364 type mature nodules, including *GASA17, GASA20* and *GASA22* and the GA repressor *DELLA-*
365 *like* (Figure 3D). This suggests that GA signalling may be somewhat suppressed in *coch*
366 nodules.

Discussion

The *COCH* gene functions as a key regulator in maintaining the developmental boundary between root and nodule identity, thereby ensuring proper nodule morphogenesis. In this study, we show that *COCH* regulates of key genes involved in cytokinin and auxin signalling, as well as genes associated with root development and nodulation in developing nodules. *COCH* controls auxin and cytokinin levels and spatial patterns of both cytokinin and auxin response during nodule development (Figure 8). In contrast, we did not find any compelling evidence that *COCH* requires gibberellin to regulate nodule formation (Figure 2D, 7). Together, these findings suggest *COCH* controls spatial hormone dynamics to specify and maintain nodule identity.

COCH suppresses cytokinin response in the developing nodule and restricts cytokinin response to specific tissue domains during nodule maturation. The ectopic cytokinin response in *coch* mature nodules may be due to elevated cytokinin levels in this tissue compared to mature wild type nodules (Figure 5A) and/or *COCH* may target cytokinin response directly, as mature *coch* nodules displayed reduced expression of several cytokinin response regulators (Figure 2D), including *PsRRB3* that is putative ortholog of *MtRRB3* that is known to promote nodule organogenesis in *Medicago* (Tan et al., 2020). Previous studies with *coch* mutants indicate that the lateral root-like outgrowths emerge from abnormal nodule vasculature meristem which has a root-related ontogeny and is derived from pericycle cell layer divisions (Magne et al., 2018b; Shen et al., 2020a). Indeed, our studies support this as we found that the activation of cytokinin biosensor *TCSn* in abnormal developing vascular tissue and tips of root-like growths of *coch* nodules (Figure 5E, G, K) is similar to the activation of cytokinin response in pea root lateral roots (Figure 5L-M) and in the provascular cells of *Arabidopsis* emerging lateral roots (Bielach et al., 2012). *COCH* is also required for establishment of cytokinin biosynthesis and response expression patterns genes during nodule organogenesis. Both cytokinin biosynthesis gene *PsIPT3* and cytokinin receptor gene *PsCHK3*, whose orthologues in *Medicago* are known to be required for nodule development (Boivin et al., 2016; Triozzi et al., 2022), fail to be up-regulated in developing *coch* nodules. Indeed, recent studies show that the expression of *MtIPT3* is specifically induced in the pericycle during nodule primordia formation to enable cytokinin biosynthesis and activation of nodule organogenesis (Triozzi *et al.*, 2022). In contrast to *Medicago*, that displayed elevated expression of cytokinin response regulator *MtRRA4* in developing nodules (Ariel et al., 2012), this was not observed for *PsRRA4* in wild type

399 developing nodules but *PsRRA4* and *PsRRA5* were ectopically expressed in developing *coch*
400 nodules.

401

402 Studies across many species indicate cytokinin influences auxin to control nodule
403 organogenesis (reviewed by Velandia *et al.*, 2022) and we found that regulation of cytokinin
404 by *COCH* was correlated with auxin level and response. Dramatically different patterns of
405 auxin response were seen between mature *coch* and wild type nodules (Figure 6, 8). Most *coch*
406 nodules displayed auxin response only in the root-like protrusions at nodule tips and on average
407 the mature nodules of *coch* mutants displayed much lower levels of auxin. However, there was
408 a range of auxin response phenotypes, including a small number of maturing *coch* nodules
409 displayed activation of auxin response throughout the nodule or in vascular strands of heart-
410 shaped nodules. This heterogeneous reprogramming of auxin response in *coch* mutants is
411 consistent with the range root-nodule hybrid phenotypes observed in *coch* nodules. The only
412 major changes in auxin gene expression in mature *coch* nodules was altered expression of
413 several auxin influx genes, including reduced expression of *PsPIN1* and *PsPIN6* and elevated
414 expression of *PsPIN4.2* and *PsPIN10* compared to wild type mature nodules (Figure 2C).
415 Recent work in *Medicago* has highlighted key roles for *MtPIN2*, *MtPIN4* and *MtPIN10* in
416 establishing the nodule meristem (Xiao et al., 2025). Thus, *COCH* may regulate correct patterns
417 of auxin transport in the maturing nodule; a key determinant of nodule initiation and
418 development (reviewed by Velandia *et al.*, 2022). Taken together, *COCH* may spatially restrict
419 cytokinin response that in turn promotes correct auxin accumulation in vascular and nodule
420 meristem to promote proper nodule development (Figure 8).

421 The *COCH* gene is essential to transcriptionally reprogram root tissue to form nodules,
422 controlling the expression of both key hormone, root and nodulation genes. Tissue specific
423 RNA-seq found that developing *coch* nodules displayed transcriptional profile that more
424 closely resemble root primordia than wild type developing nodules (Figure 3B),
425 complementing previous studies in *Medicago* that found *noot noot2* mutants failed to regulate
426 around 40% of genes that wild type plants differentially expressed within 24-72 hours of
427 inoculation with rhizobia (Lee *et al.*, 2024). We found even larger divergences in expression
428 between *coch* and wild type occur in the developing nodule tissue (Figure 3, Figure S2). *COCH*
429 is required during early nodule development to suppress expression of auxin biosynthesis,
430 transport, perception and response genes (nine *AUX/IAA* repressors, four *ARFs*, and two
431 *AUX1/LAX* transporters). Several of these genes have homologs in other species that are known

432 to regulate lateral root development; *ARF8* promotes lateral roots and *IAA14* suppresses lateral
433 roots in *Arabidopsis* (Fukaki et al., 2005; Fukaki et al., 2002; Wang et al., 2015) and in soybean
434 *GmARF8* must be locally suppressed to enable nodules to form (Wang *et al.*, 2015). Notably,
435 auxin-regulated transcription factors *PLT3* and *PLT5* involved in root apical meristem
436 maintenance and differentiation and correct formation and patterning of lateral roots (Du and
437 Scheres, 2017; Galinha et al., 2007; Hofhuis et al., 2013; Mähönen et al., 2014) fail to be up-
438 regulated in *coch* developing nodules and are downregulated in mature *coch* nodules
439 respectively. In contrast, several other genes with important roles in lateral root development
440 *HB2*, *GRF6* and members of the *KNOX* family (Dean *et al.*, 2004; He *et al.*, 2020; Qi and
441 Zheng, 2013; Rodriguez *et al.*, 2015; Truernit and Haseloff, 2007; Yan *et al.*, 2024), are up-
442 regulated in *coch* developing or mature nodule compared to wild type (Figure S2C). The
443 majority of nodulation genes upregulated in wild type developing nodules fail to be upregulated
444 in developing *coch* nodules, although their expression is restored in mature *coch* nodules
445 (Figure S2D). Therefore, *COCH* may act upstream of cytokinin and auxin early in nodule
446 development to maintain nodule identify by suppressing key root identity genes and promoting
447 key nodulation genes and this sets the organs on a nodule trajectory.

448 *PsCOCH* appears to act specifically in the root to influence nodule organogenesis, with no
449 consistent effects on rhizobial infection, root architecture or colonisation with arbuscular
450 mycorrhizal fungi (Figure 1, Figure S1, Table S2). The fact that no change in root architecture
451 was detected in *coch* mutants is consistent with no major changes in gene expression in root
452 primordia of wild type and *coch* mutant lines (Figure 3A). The only interaction of *COCH* with
453 rhizobial infection was the reduced cytokinin response associated with *coch* infections
454 compared to wild type (Figure 6). The hyperinfection phenotype displayed by gibberellin-
455 deficient *na* mutants is known to be associated with ectopic cytokinin response (Velandia *et*
456 *al.*, 2024), so the observed suppression of cytokinin response in *coch* mutants might be why *na*
457 *coch* double mutants displayed attenuation of infection thread formation and branching (Figure
458 7A). In addition to playing a key role in nodule organogenesis, *COCH* also promotes bacterial
459 occupancy of the nodules as the infection and fixation zones of *coch* nodules contain less
460 bacteria (e.g. Figure 1E and 5K) and *coch* mutants fix less nitrogen (Liu *et al.*, 2023). This may
461 be due to upregulation of defence-related genes (Figure S2B) and mis-regulation of genes with
462 key roles in symbiosome formation such as *DNF1*, *SYT* and *VAMP72* (Gavrin et al., 2017;
463 Ivanov et al., 2012; Van de Velde et al., 2010; Wang et al., 2010)(Figure S2D).

464 Interestingly, both loss-of-function mutations and overexpression of *COCH* throughout the root
465 lead to the formation of root-like structures emerging from nodules (Figure 4), indicating that
466 *COCH* function is dosage-sensitive and must be tightly regulated during nodule development.
467 This dual phenotype suggests that *COCH* is not merely required to initiate nodules or suppress
468 root identity but rather plays a central role in stabilizing and maintaining the nodule
469 developmental program. Overexpression of *COCH* may perturb downstream regulatory
470 networks or disrupt the balance between auxin and cytokinin signalling pathways, resulting in
471 aberrant organ identity similar to that observed in loss-of-function mutants. Such
472 developmental alterations caused by ectopic expression of homeotic proteins have previously
473 been demonstrated for *KNOX*, *WUSCHEL*, and *PLETHORA* (Aida et al., 2004; Chuck et al.,
474 1996; Gallois et al., 2004).

475 The negative regulation of nodule number via AON pathway is thought to be triggered by
476 formation of mature nodules (Kassaw *et al.*, 2015; Li *et al.*, 2009) and has been suggested to
477 act via upregulation of *TML* transcriptional regulator (reviewed by Scott et al., 2024). The fact
478 that *coch* mutants do not produce more nodules than wild type and that there was no additive
479 phenotype in *coch* AON double mutants (Figure 2) indicates the root-nodule hybrids of *coch*
480 mutants can still activate the AON pathway to control nodule number. The failure to induce the
481 expression of *TML2* in mature *coch* nodules (Figure S2D) did not correlate with an increase in
482 nodule number in *coch* mutants and this is consistent with evidence in *Medicago* showing that
483 regulators in addition to TML control nodule number (Schnabel et al., 2023). Interestingly
484 however, we did observe that *coch Psnark* and *coch clv2* double mutants generated a higher
485 proportion of abnormal nodules than *coch* single mutant background. In pea, *Ps*NARK (CLV1)
486 and *Ps*CLV2 putative CLE receptors play a role in regulating shoot meristem proliferation
487 (Scott *et al.*, 2024) but these genes did not have an obvious effect on root development (Wang
488 *et al.*, 2020). However, in other legumes CLV1 orthologs have been shown to suppress lateral
489 root development (Goh *et al.*, 2018; Lagunas *et al.*, 2019; Wopereis *et al.*, 2000). The additive
490 root-nodule phenotype of *coch Psnark* and *coch clv2* double mutants indicates *Ps*NARK and
491 *Ps*CLV2 may interact with the root program by suppress root identity in developing nodules.
492 Indeed, the upregulation of *KLV1* and *KLV2* expression in developing *coch* nodules (Figure
493 S2D) suggests other potential cross overs between AON pathway and COCH. KLV is a shoot
494 acting receptor that suppresses nodule number and also promotes lateral root formation in *Lotus*
495 (Miyazawa et al., 2010; Oka-Kira et al., 2005) and the KLV ortholog in *Arabidopsis*
496 *TOAD2/RPK1* suppresses root meristem proliferation (Racolta et al., 2018). Thus, upregulation

497 of *PsKLV1* and/or *PsKLV2* in *coch* nodules may enhance the formation of root-like tissue.
498 These observations point to a broader regulatory role for CLE peptide receptors in organ
499 identity and morphogenesis in root tissues, possibly by acting downstream of COCH. It would
500 be interesting to explore if similar interactions between COCH and CLE peptide signalling
501 occur in the shoot, as both pathways also control shoot organ identity.

502 Taken together, our findings provide direct evidence that COCH, modulates cytokinin and
503 auxin pathways at multiple levels—transcriptional regulation, hormone levels, and spatial
504 hormone response—to direct nodule formation and preserve nodule identity (Figure 8). In our
505 studies RNAseq and hormone analysis were analysed at organ level and hormone response was
506 spatially delineated, in the future it would be enlightening to monitor spatial levels of
507 transcription and hormone level to resolve the precise mode of action of *COCH* to regulate
508 hormone dynamics during nodule development. Members of the NBCL gene family, including
509 COCH, function as transcriptional co-regulators that influence the development of diverse
510 shoot organs—such as leaves, flowers, and inflorescences—across monocots and dicots, both
511 legumes and non-legumes (Couzigou *et al.*, 2012; Khan et al., 2014; Liu *et al.*, 2023; Magne
512 *et al.*, 2018a) and it would be interesting to explore if COCH regulates common targets in auxin
513 and cytokinin pathways to shape shoot development.

514

515 **Methods**

516 **Plant material, germplasm generation and growth conditions**

517 The *Pisum sativum L.* lines used in this study were *coch-JI216* and *coch-JI2757* and their
518 respective wild type lines cv. Weitor and Parvus (Blixt, 1967; Couzigou *et al.*, 2012). The
519 gibberellin-deficient mutant *na-1* derived from WT line WL1769 (Davidson et al., 2003),
520 *Psnark* (P88, formerly *sym29*, disrupted in *PsCLV1*) and *Psclv2* (P64, formerly *sym28*) derived
521 from the parental line 'Frisson' (Duc and Messager, 1989; Krusell et al., 2002; Krusell et al.,
522 2011; Sagan and Duc, 1996; Schnabel et al., 2011). The double mutant line *na coch* were
523 generated from cross between *coch-JI2165* and *na-1*. The double mutant lines *Psnark coch* and
524 *Psclv2 coch* were generated from cross between *coch-JI2165* and *Psnark* or *Psclv2*. Double
525 mutant, single mutants and wild type derivatives from these crosses were selected in the F2
526 generations using reduced stipules phenotype to select *coch,* dwarfism for *na* and RFLP
527 markers to select *Psnark* or *Psclv2*. Primers for PCR amplification of template are listed in
528 Table S1. Restriction digests were carried out using BsmAI for *PsNARK* and BtsCI for *PsCLV2*.

529 Unless otherwise stated plants were grown in glasshouse conditions as described by Foo and
530 Davies (2011) in sterile conditions and inoculated at day 7 with *Rhizobium leguminosarum* bv
531 *viciae* strain RLV248 containing the plasmid Phc60 for GFP constitutive expression
532 (RLV248G) (Cheng and Walker, 1998) as described by Velandia *et al.* (2024) and received
533 modified Long Ashton nutrients with no nitrogen weekly (Hewitt, 1966). To characterise root
534 architecture of *coch* lines, plants were grown with respective wild type progenitors in sterile
535 conditions for 28 days and received sterile Long Ashton nutrients with no nitrogen 14 and 20
536 days after planting. For AM study, plants were inoculated with *Rhizophagus irregularis* and
537 grown with modified Long Ashton nutrients with 10 mM KNO3 and 0.05 mM NaH_2PO_4
538 weekly as outlined in Foo et al. (2013).

539

540 **Examination of nodulation structures and root architecture**

541 For nodulation experiments in AON *coch* double mutants, plants were harvested 3 weeks after
542 rhizobial inoculation and nodules were scored by eye and classified as mature nodule (typical
543 mature pea nodule) or root-nodule hybrid (with protruding root-like structures characteristic of
544 coch mutant; Ferguson and Reid, 2005). For all other experiments roots were examined using
545 a Zeiss Axioscope5 fluorescence microscope. The total number of IT, developing nodules (not
546 yet emerged from the root profile), mature nodules and abnormal nodules (including root-
547 nodule hybrids) were counted per cm of root length. For *na coch* mutants, branched IT were
548 also counted and due to the reduced root length of plants carrying the *na* mutation structures
549 were expressed the number of structures per cell as outlined in Velandia *et al.* (2024) . For
550 *TCSn::GUS* transformation experiments the presence of GUS staining associated with each
551 structure was also recorded. Root architecture was examined in Table S2 was performed
552 measuring the length of the top 6 secondary roots, the number of tertiary roots on the longest
553 secondary root and the length of the longest tertiary root on the longest secondary root.

554 **Construct assembly and hairy root transformation**

555 Specific promoters and genes where inserted in the Pcambia_CR1 (PCR1) vector (Sevin-Pujol
556 et al., 2017) using Golden Gate system, following the instructions of Golden Gate assembly kit
557 (New England Biolabs). The *PsCOCH* coding region (Psat3g077680) (1467bp) was obtained
558 from pea root cDNA. The *AtCASP1* endodermal promoter (Roppolo et al., 2011) and *CO2*
559 promoter, were obtained directly from a PBS plasmid kindly provided by Sandra Bensmihen
560 (Sevin-Pujol *et al.*, 2017). The two component signalling (*TCSn*) cytokinin responsive

561 promoter was supplied by Bruno Muller (Zürcher et al., 2013) and was linked to the *GUS*
562 reporter in the PCR1 vector. The *DR5* promoter was obtained from the pGreenIIM DR5v2-
563 ntdTomato/DR5-n3GFP (Liao et al., 2015) and fused with *GUS* reporter gene in the PCR1
564 vector. PCR fragments for *TCSn, DR5* and *35S* promoter regions and *GUS* and *COCH* genes
565 where generated using primers containing the BsaI recognition site and matching overhangs
566 (Table S1). Pea roots were transformed with *Agrobacterium rhizogenes* (ARqua1) carrying the
567 corresponding construct according to Velandia *et al.* (2024). Plants were harvested three weeks
568 post rhizobial inoculation. For harvesting, individual roots regenerated from the callus of 10–
569 20 plants were screened for transformation using the DsRED fluorescent marker. Transformed
570 roots were then fixed in 1% paraformaldehyde and stored at 4 °C for subsequent scoring. For
571 *TCSn* and *DR5* studies, roots were stained for GUS before fixation in paraformaldehyde as
572 described in Velandia *et al.* (2024).

573 **Root sectioning**

574 Roots were removed from paraformaldehyde, trimmed and placed into 2.5M sucrose overnight.
575 Tissue was embedded in 1:1 mixture of 2.5M sucrose:OCT (Scigen) in a cryostat mold, snap
576 frozen and 16µm sections were made using Epredia Cryostar HM525 NX (Epredia, UK).
577 Sections were briefly rinsed in water and mounted on slides.

578 **RNA seq studies**

579 Wild type (Weitor) and *coch JI-2165* plants were inoculated with RLV248G 14 days after
580 planting and grown under glasshouse conditions as described. When plants were 6 weeks old,
581 roots were washed and for each genotype three tissue types were harvested; root tips,
582 developing nodules (< 2mm in size, with a small amount of mature root attached) and mature
583 nodules (> 2mm in size, with a small amount of mature root attached). In *coch* plants, mature
584 nodules consisted of root–nodule hybrids along with a few visually normal nodules. For each
585 tissue type and genotype combination, four biological replicates were collected, each
586 comprising tissue from 2–3 plants. Additional replicate samples of mature nodules were
587 collected separately for hormone analysis, as described below. Tissue was frozen in liquid-N
588 and RNA was extracted using ISOLATE II RNA mini kit (Bioline). RNA samples were
589 processed for mRNA library preparation (poly(A) enrichment) and sequenced on a NovaSeq X
590 Plus platform (PE150) by NovogeneAIT (Singapore). Quality control assessment of the RNA-
591 seq data was conducted using the FastQC tool (Andrews, 2017). Based on the quality control
592 analysis, reads were subsequently processed using Trimomatic (Bolger and Giorgi, 2014). The
593 sequences underwent pseudoalignment against the pea (*Pisum sativum*) Cameor transcriptome

(Alves-Carvalho et al., 2015) using Kallisto (Bray et al., 2016). The differential expression analysis was done using Sleuth package (Pimentel et al., 2017) and the differentially expressed genes were obtained by pairwise comparison of each treatment against the wild type root primordia treatment as a control. The selection of DEGs was based on the false discovery rate corrected p-values under 0.05 and $\log_2$ fold of change over 1. GO enrichment analysis was performed using TopGO package (Alexa et al., 2006).

Hormone analysis

Auxin and cytokinin extraction and quantification was carried out as outlined in Bound et al. (2022) with stable isotope-labelled internal standards added to each sample. Samples were then analysed using a Waters Acquity H-Class UPLC instrument coupled to a Waters Xevo triple quadrupole mass spectrometer. For all samples, peak areas for endogenous and labelled hormones were compared and combined with the FW of samples to calculate ng/g FW.

Funding

All authors were supported by the Australian Research Council Centre of Excellence for Plant Success [grant numbers CE200100015 and DP190101817].

Author contributions

E.F. conceived the project. N.S., T.S., K.V., A.C., A.M, and E.F. performed the experiments and analysed the data. E.F wrote the manuscript with input from all authors.

Acknowledgements

We thank Maria Soto (University of Granada) for the gift of GFP-labelled *Rhizobium*, Sandra Bensmihen (INRA, France) for the *pCAMBIA CASP* and *CO2* construct, Bruno Mueller (Zurich-Basel Plant Science Center, Department of Plant and Microbial Biology, UZH) for the *TCSn* promoter, and David Nichols (CSL, UTAS) for expert assistance with hormone analysis. We thank Tracey Winterbottom and Sarah Kane for assistance with plant husbandry.

Declaration of interests

The authors declare no competing interests.

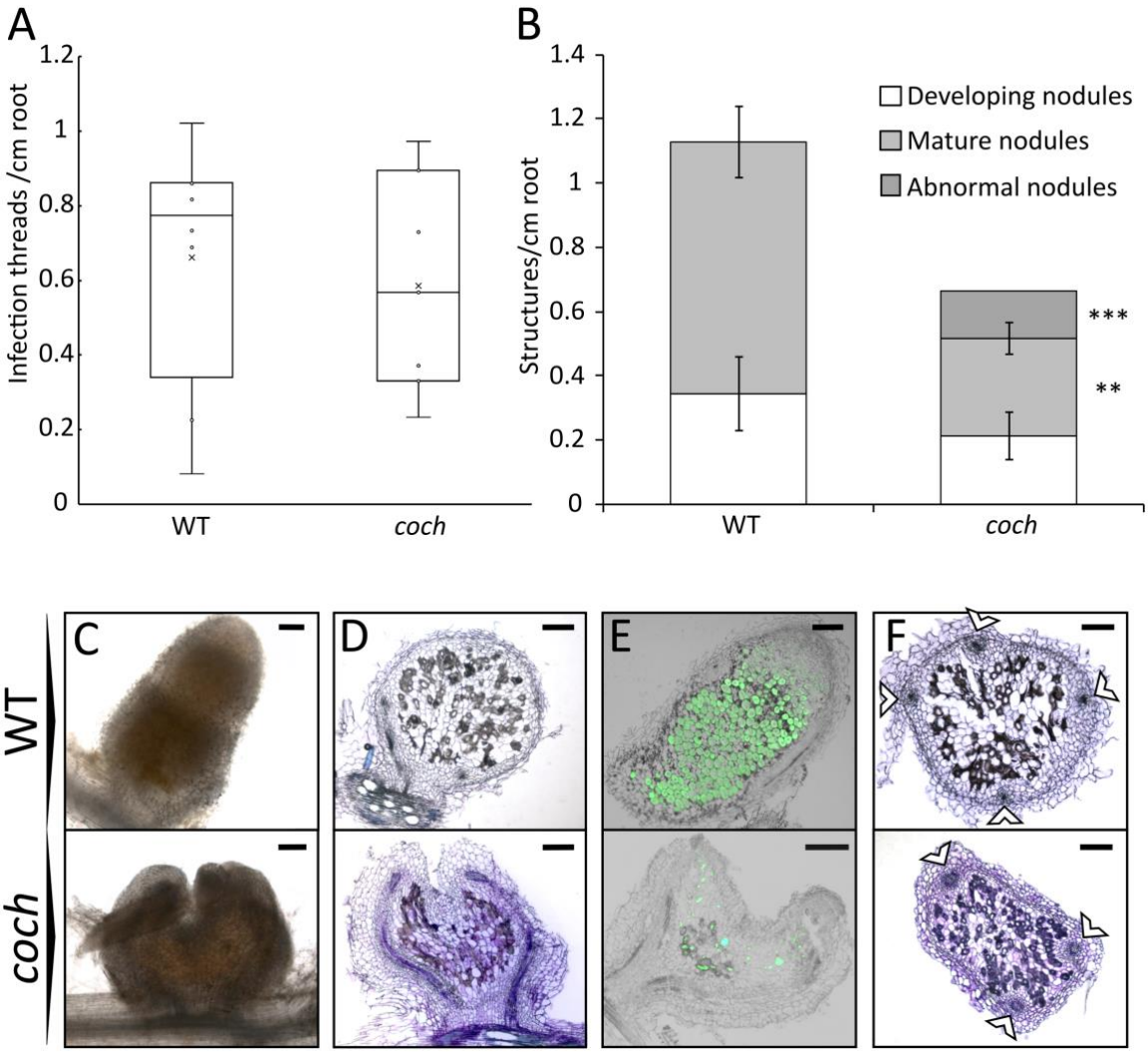

Figure 1. Nodule development defects in the *coch* mutant include root-like structures, reduced colonization, and vascular disorganization.

Nodulation phenotypes of wild-type Weitor (WT) and *coch*-JI2165 mutant plants at 6 weeks old, 4 weeks after rhizobial inoculation

(A) Number of infection threads per cm of root length. Boxes represent the interquartile range, horizontal lines show the median, and whiskers indicate the full data range.

(B) Number of nodules per cm of root length. Data in (A–B) represent mean ± standard error (SE), $n = 7$. Asterisks indicate statistical significance based on *t-test*: $^{**}p < 0.01$, $^{***}p < 0.001$.

(C) Brightfield microscopy images of typical nodules in wild-type and *coch* mutant plants, showing an abnormal nodule with a root-like structure at the tip in the mutant. (D) Longitudinal sections of wild-type and *coch* mutant nodules, showing the characteristic heart-shaped morphology in the mutant.

(E) Brightfield and GFP-fluorescence merged images of longitudinal sections showing GFP-tagged *Rhizobium leguminosarum* within nodules.

(F) Transverse sections of wild-type and *coch* mutant nodules under brightfield microscopy, with white arrows indicating vascular bundles. Scale bars = 200 µm. (D, F) Sections were stained with toluidine blue.

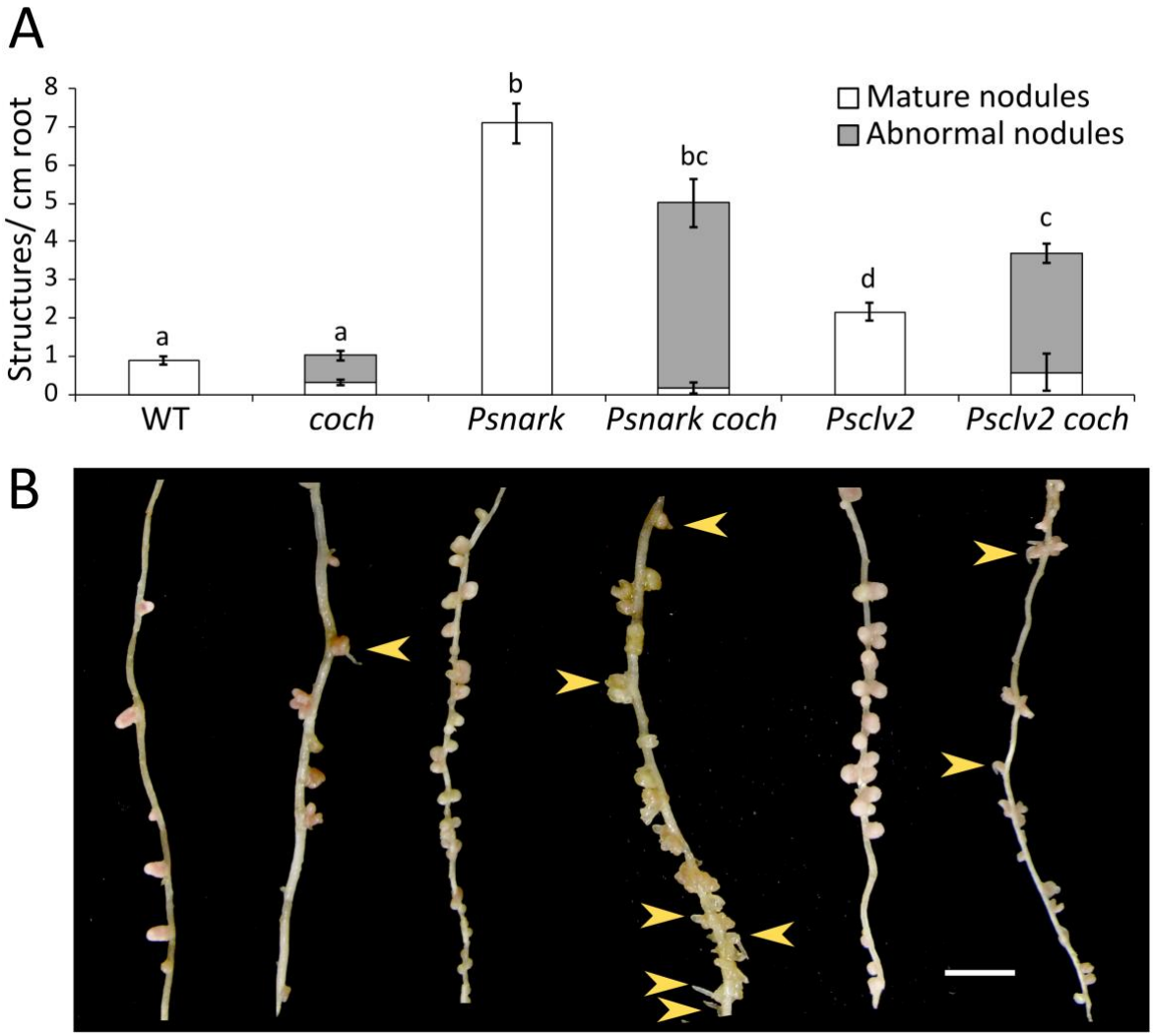

Figure 2. Double *coch*-AON mutants develop a higher proportion of abnormal nodules compared to single mutants and wild type.
(A) Number of mature, normal, and abnormal nodules per cm of root in wild-type plants, single mutants, and F3 double mutant segregants from a cross between *coch-JI2165* and *Psnark Psclv2*. Data are shown as mean ± SE, $n = 5–6$. Different letters indicate statistically significant differences in total nodule number (mature + abnormal), assessed using Tukey's Honestly Significant Difference (HSD) test ($p < 0.05$).

(B) Representative root images showing typical secondary roots. Yellow arrows indicate abnormal nodules displaying root-like outgrowths at the tip. Scale bar = 1 cm. Plants were grown for 4 weeks, and nodulation phenotypes were assessed 3 weeks post-inoculation with *Rhizobium*.

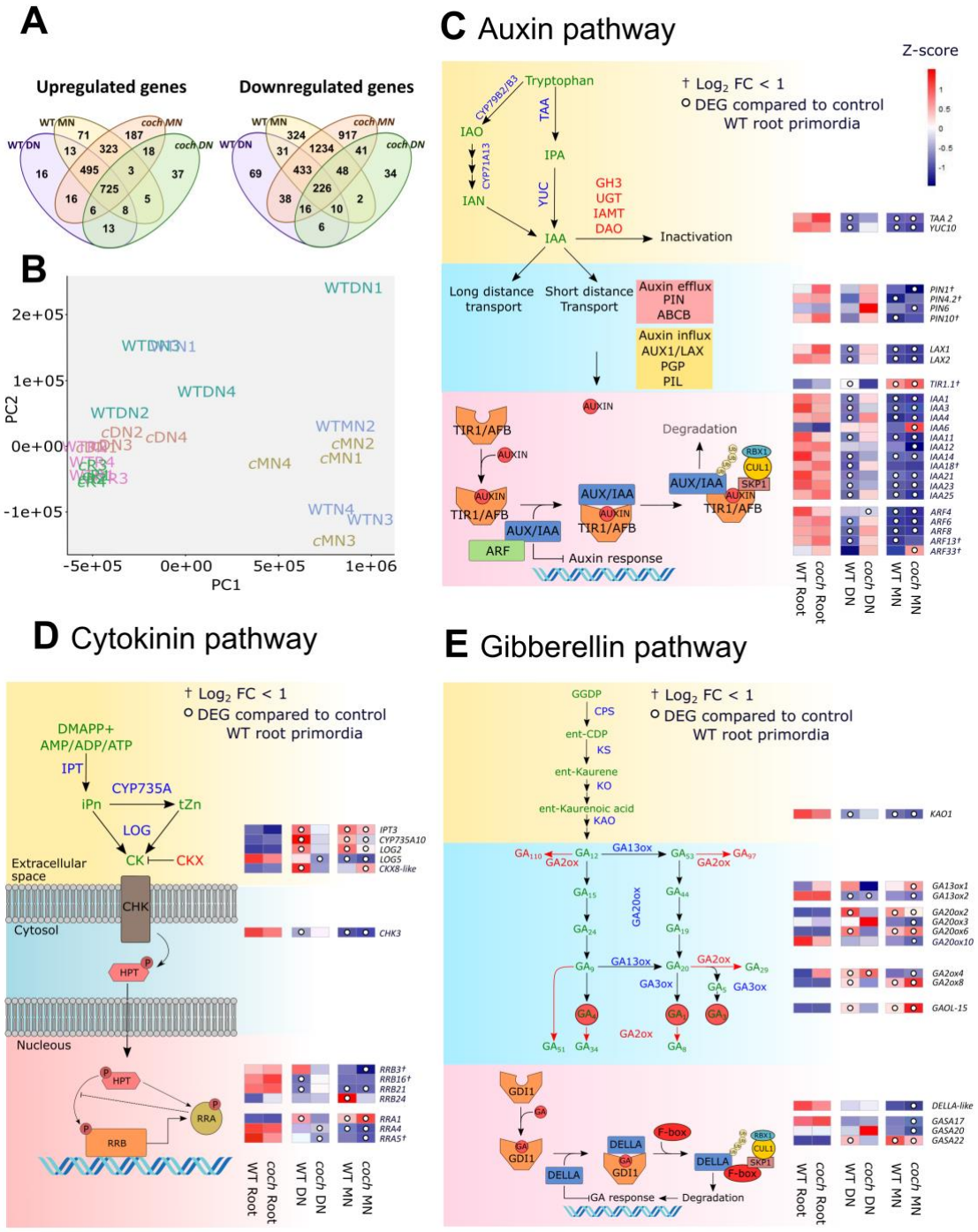

Figure 3. Transcriptomic comparison of wild-type and *coch* mutant nodules reveals hormone pathway alterations.

(A) Venn diagram showing the overlap of differentially expressed genes (DEGs) that were upregulated or downregulated in wild-type and *coch* mutants in developing and mature nodules.

(B) Principal component analysis (PCA) of gene expression profiles across samples. Each point represents a biological replicate (n = 4).

(C–E) Simplified hormone pathway diagrams and heatmaps showing expression patterns of genes involved in auxin (C), cytokinin (D), and gibberellin (E) biosynthesis, signalling, and catabolism. Hormone species and intermediates are shown in green, biosynthesis enzymes in blue, and catabolic enzymes in red. Arrows indicate enzymatic reaction directionality. Only genes showing a differential expression pattern between wild-type and *coch* mutants are included in the heatmaps. The heatmap colour scale represents Z-scores of normalized gene expression. White circles within each heatmap cell indicate that the gene in that specific condition was significantly differentially expressed relative to the wild-type root primordia (q-value < 0.05). Genes marked with a cross (†) indicate that although differentially expressed, their absolute $\log_2$ fold change ($\log_2$FC) was < 1.

Samples were collected from 6-week-old plants, 4 weeks post-inoculation with *Rhizobium*. Tissues included root tips, developing nodules, and mature nodules for wild-type, and abnormal nodules for *coch* mutants.

Abbreviations: $DMAAP^+$: N6-(Δ2-isopentenyl)adenosine monophosphate. AMP/ADP/ATP: Adenosine mono/di/tri-phosphate. iPn: Isopentenyladenine. tZn: *Trans*-zeatin. CK: Cytokinin. IAO: Indole-3-acetaldoxime. IAN: Indole-3-acetonitrile. IPA: Indole-3-pyruvic acid. IAA: Indole-3-acetic acid. GGDP: Geranylgeranyl diphosphate. *ent-CDP*: *ent*-Copalyl diphosphate. GA: Gibberellin. DN: Developing nodule. MN: Mature nodule. Gene symbols and full names are listed in Table S3.

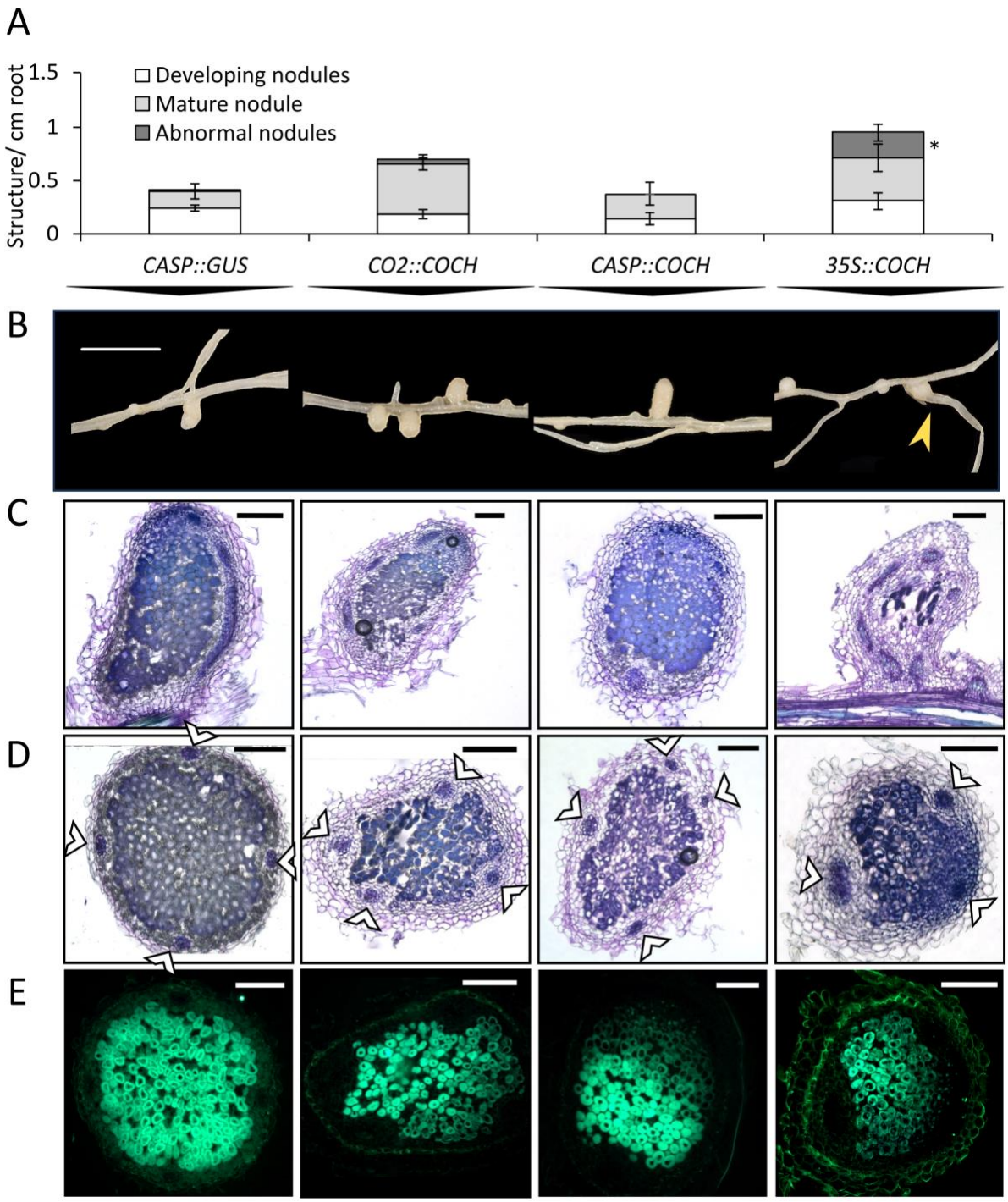

680

681 **Figure 4. Ectopic expression of *PsCOCH* in hairy roots induces abnormal nodules and**
682 **nodule–root hybrids in wild-type *Parvus*.**
683 Nodulation phenotypes were assessed 3 weeks post-inoculation in hairy root-transformed wild-
684 type *Parvus* plants expressing *PsCOCH* under a constitutive promoter (*35S::COCH*), an
685 endodermis-specific promoter (*CASP::COCH*), or a meristem-specific promoter
686 (*CO2::COCH*). Plants transformed with *CASP::GUS* (endodermis-specific promoter driving
687 β-glucuronidase) were used as controls.

688 (A) Number of developing, mature, and abnormal nodules per cm of root. Data represent mean
689 ± SE, n = 8–9. $p < 0.05$ (t-test).

690 (B) Images of root segments showing representative nodules from each transformation
691 condition. Scale bar = 2 cm.

692 (C) Longitudinal sections of representative nodules from each treatment stained with toluidine
693 blue.

694 (D–E) Transverse sections of representative nodules stained with toluidine blue, shown in
695 brightfield (D) and GFP fluorescence (E). GFP indicates *Rhizobium leguminosarum*. White
696 arrows (D) indicate vascular bundles. Scale bars = 200 μm.

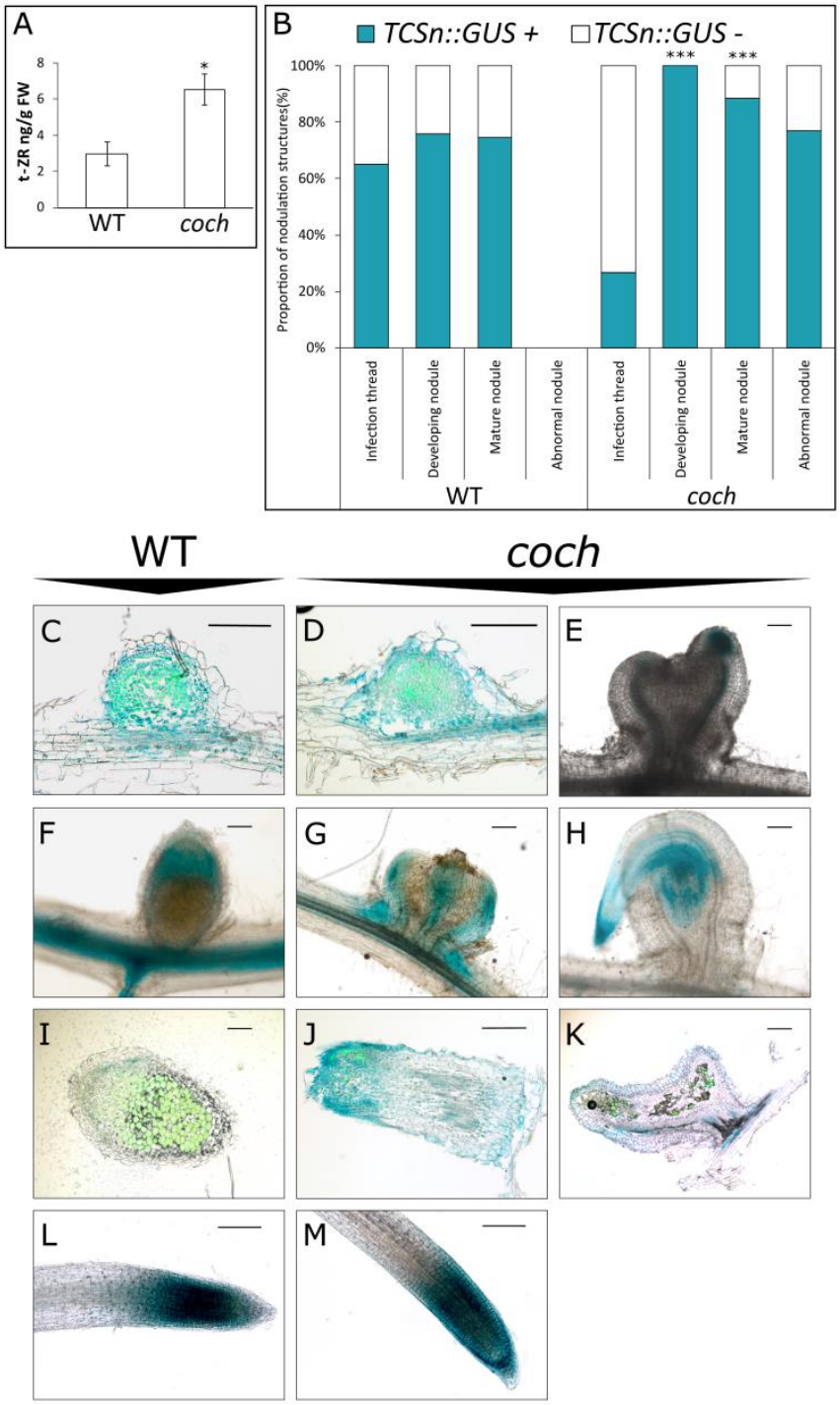

Fig. 5. Cytokinin response and levels are elevated in *coch* abnormal nodules. Cytokinin accumulation and cytokinin-responsive promoter activity were assessed in *coch-JI2165* and wild-type *Weitor* (WT) roots transformed via hairy root transformation with the cytokinin reporter construct *TCSn::GUS* (a synthetic cytokinin-responsive promoter driving *β*-glucuronidase expression).

(A) Quantification of *trans*-zeatin riboside (t-ZR) levels in mature nodules of WT and *coch*. Data are mean ± SE, $n = 4$. Asterisk indicates significant difference ($p < 0.05$, *t*-test).

705 (B) Proportion of infection and nodule structures showing *TCSn::GUS* activity (*TCSn::GUS*+)
706 or no detectable activity (*TCSn::GUS*−) in WT and *coch*. Chi-squared test was performed for
707 each structure type; ***$p < 0.001$, $n = 6–7$.

708 (C–M) Representative microscopy images of *TCSn::GUS* expression in various tissues. Blue
709 indicates GUS activity; GFP fluorescence marks *Rhizobium leguminosarum* colonization.

710 (C–D) Longitudinal sections of developing nodules

711 (E–H) Whole mature nodules

712 (I–J) Longitudinal sections of mature WT nodule and abnormal *coch* nodule

713 (L–M) Root tips expressing.

714 Scale bars = 200 µm for all panels. Roots were sampled from 4 weeks post-*Rhizobium*
715 inoculation.

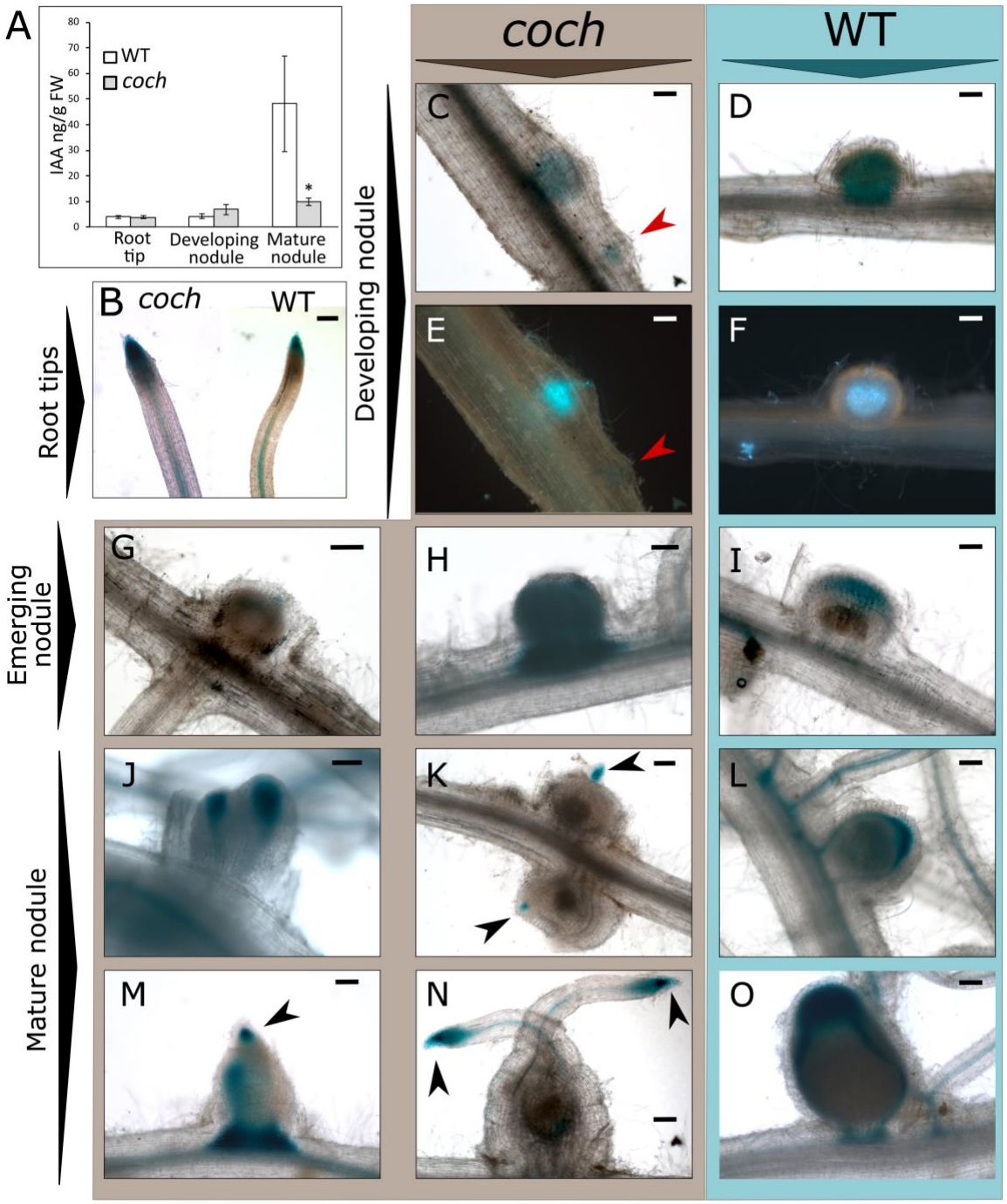

716

717 **Fig. 6. Auxin levels are reduced, and auxin response is altered in *coch* abnormal nodules.**
718 Auxin accumulation and auxin-responsive promoter activity were evaluated in *coch-JI2165*
719 mutants and wild-type *Weitor* (WT) roots transformed via hairy root transformation with the
720 DR5::GUS reporter construct (a synthetic auxin-responsive promoter driving *β*-glucuronidase
721 expression).

722 (A) Indole-3-acetic acid (IAA) content (ng/g fresh weight) in root tips, developing nodules,
723 and mature nodules of WT and *coch*. Data are shown as mean ± SE, $n = 4$; $p < 0.05$ (Student's

724 *t*-test).

725 (B–O) Microscopy images showing DR5::GUS activity in root tissues of WT and *coch-JI2165*.
726 Blue staining indicates GUS activity (auxin response), green fluorescence indicates *Rhizobium*
727 *leguminosarum* expressing GFP.

728 (B) Representative root tips

729 (C–F) Developing nodules in brightfield (C–D) and GFP fluorescence (E–F); red arrows
730 indicate root primordia

731 (G–H) Older developing nodules

732 (J–O) Mature nodules; black arrows indicate root-like structures at the tips of abnormal *coch*
733 nodules

734 Scale bars = 200 µm for all panels. Tissues were sampled 4 weeks after *Rhizobium* inoculation.

735

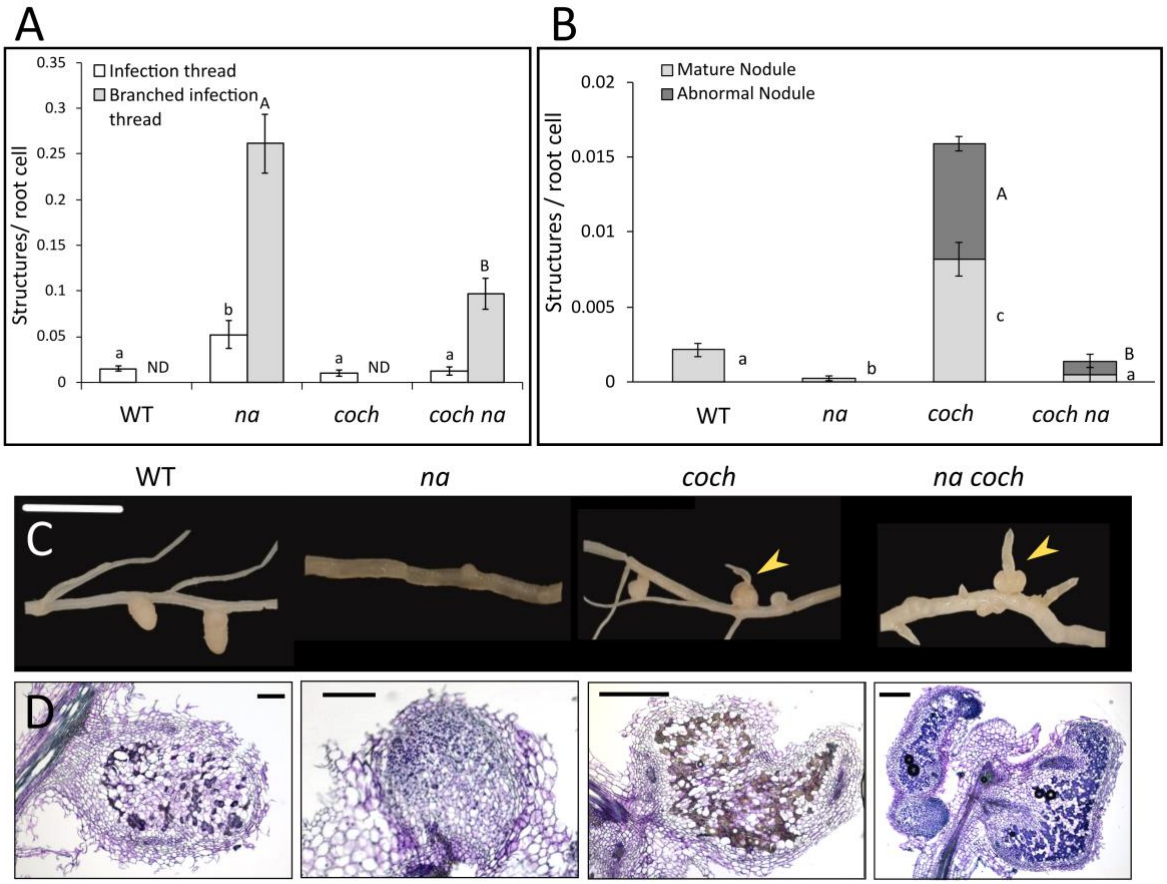

Fig 7. Gibberellin is not required for the formation of root-nodule abnormal structures in *coch* mutants. (A-B) Nodulation phenotypes of four weeks old F_3 segregants from cross between *coch-JI2165* and gibberellin deficient *na* mutant, evaluated 3 weeks post inoculation.

(A) Number of infection threads and branched infection threads

(B) Number of normal and abnormal nodules per root cell, bars are mean ± SE, n = 5-6. Within a parameter, values with different letters are significantly different $p < 0.05$. ND not detected.

(C) Photo of typical secondary root, yellow arrows indicate abnormal nodules with clear roots at tip. Scale bar is 2cm.

(D) Longitudinal sections of nodules stained with tolidine blue; scale bar is 200µm.

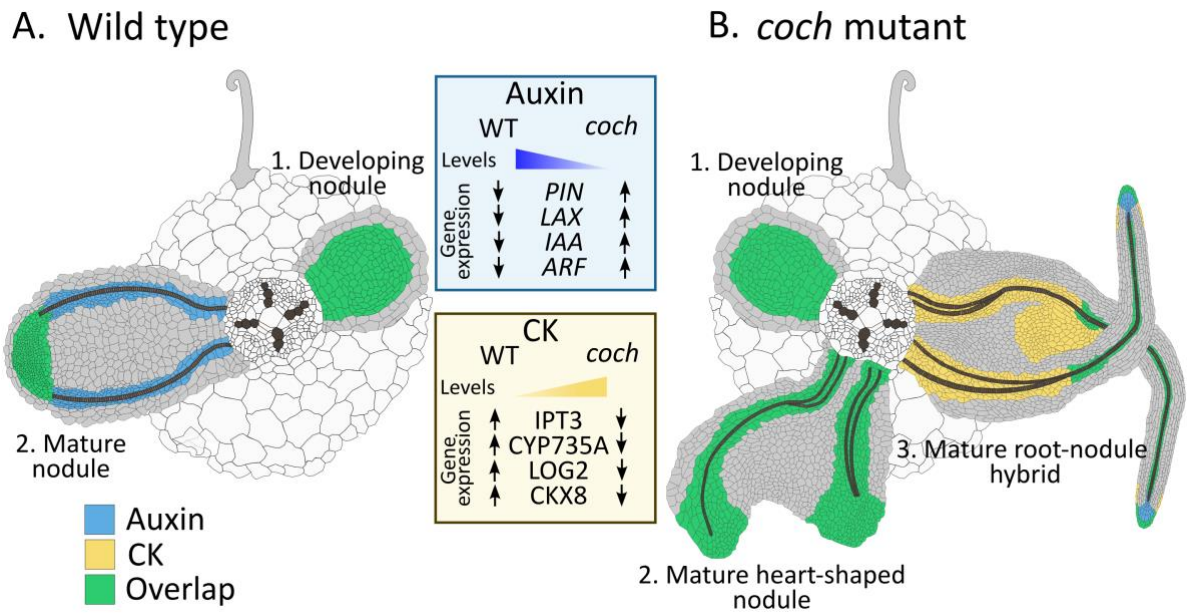

Figure 8. Model of hormone levels, gene expression, and spatial response of auxin and cytokinin in wild-type and *coch* mutant nodules.

The spatial patterns of auxin and cytokinin response are illustrated for developing and mature nodules in wild-type and *coch* mutants. In wild-type plants, auxin and cytokinin responses overlap in the emerging nodule (A1) and remain co-localized in the meristematic region of mature nodules (A2), with auxin response also present in the nodule vasculature. In *cochleate* mutants, developing nodules initially display an overlapping auxin and cytokinin response (B1), similar to the wild type, but subsequently develop into either heart-shaped nodules (B2) or root–nodule hybrids (B3). In heart-shaped nodules, both auxin and cytokinin responses are maintained in the vasculature and at the lobe tips, but are lost from the apical meristematic region. In root–nodule hybrids, auxin response is strongly reduced and restricted to the vasculature and the tips of the fused roots, whereas cytokinin response is broadened and intensified, particularly in the abnormal vasculature and the apical zone between the merged roots. These spatial patterns are consistent with hormone quantification, which show that auxin levels are reduced in *cochleate* abnormal nodules while cytokinin levels are elevated. Gene expression analysis revealed that that auxin transport and response genes are upregulated in *coch*, and that cytokinin biosynthesis and catabolism genes are downregulated in the mutant.

769 **Supporting Information**

770 **Supplementary Table 1. List of primers used for Golden Gate assembly, qPCR, and RFLP**
771 **analysis.** This table includes the sequences and relevant notes for primers used in Golden Gate
772 cloning, quantitative Polymerase Chain Reaction (qPCR), and restriction fragment length
773 polymorphism (RFLP) analysis. Primer sequences are listed in the 5′ to 3′ direction.

774 *Due to the highly repetitive nature of the pGreenIIM DR5v2-ntdTomato/DR5-n3GFP
775 construct, an internal region containing the promoter was first amplified using flanking primers
776 designed outside the repetitive sequence. This PCR product was then used as a template for
777 amplification with Golden Gate-compatible primers for subsequent cloning: DR5-flank-F :
778 ACCTGTTCCTGGGGCATG, DR5-flank-R : CTTGCTCACCATGGATCTCT.

779 ** Fragments were domesticated prior to cloning to remove an internal BsaI restriction site.

780

Target	Primer	Use
DR5 promoter F*	GGCTACGGTCTCCAAATTATCGCGCGCGGTGTCAT	Golden gate cloning
DR5 promoter R*	GGCTACGGTCTCGTTTGAGCCATGGATCCCCTGTAATTG	Golden gate cloning
TCSn F	GGCTACGGTCTCGAAATAAGCTTGACTAGTCAAAG	Golden gate cloning
TCSn R	GGCTACGGTCTCTTTTGTGTTATATCTCCTTGGATCG	Golden gate cloning
β-glucuronidase (GUS) F	GGCTACGGTCTCTCAAATGTTACGTCCTGTAGAAAC	Golden gate cloning
β-glucuronidase (GUS) R	GGCTACGGTCTCCCGTATCATTGTTTGCCTCCCTGC	Golden gate cloning
35S promoter F**	GGCTACGGTCTCGAAATGAGCTCTCCCATATGGTC	Golden gate cloning
35S promoter R**	GGCTACGGTCTCGTTTGTGATATCACTAGTGCGGC	Golden gate cloning

PsCOCH F**	GGCTACGGTCTCTCAAAATGTCCCTTGAAGACTCC	Golden gate cloning
PsCOCH R**	GGCTACGGTCTCTCGTATTAGTAGTCATGAGAATGATGATG	Golden gate cloning
PsCOCH qPCR	GCA TTG CTC ACT CAG AAA CAA C	qPCR
PsCOCH qPCR	AGA CCA GAT TTC GCG ACG AG	qPCR
PsTFIIa qPCR F	CGGTGGAAATGCTGATGTA	qPCR
PsTFIIa qPCR R	GCTCCCTCCACATACCTCAA	qPCR
PsActin qPCR F	ATTGCATTGCACTTTGTGTAGCC	qPCR
PsActin qPCR R	CCATCTTTTACAAAAACGTGAAA	qPCR
PsNARK RFLP F	GAA ATT CCA CCG AGT TTT GG	RFLP
PsNARK RFLP R	CAA TCC GGT GAG GTG ATT CT	RFLP
PsCLV2 *RFLP* F	TGCAGGCTTTGTTCCTTTC	RFLP
PsCLV2 *RFLP* R	ACCGGGAAATCTTCCATACC	RFLP

781

782

783 **Supplementary Table 2. Root phenotypes of *coch*-JI2165 and *coch*-JI2757 mutants and**
784 **their corresponding isogenic wild-type lines, Weitor and Parvus.**

785 Plants were grown under sterile conditions for 28 days. Values are presented as mean ± standard
786 error (SE), $n = 10–16$. Asterisks indicate statistically significant differences from the respective
787 wild-type line, based on Student's *t*-test (*$p < 0.05$; **$p < 0.01$).

788 The length of secondary roots corresponds to the average length of the six longest secondary
789 roots. The number of tertiary roots was counted on the longest secondary root. The length of
790 the tertiary root refers to the longest tertiary root on that same secondary root.

791

Genotype	Tap root length (cm)	Length secondary root (cm)	No. secondary roots/cm tap root	No. tertiary roots/cm secondary root	Length tertiary root (cm)	Shoot DW (mg)	Root DW (mg)	Shoot:root ratio
Weitor	20.3 ± 1.5	18.1 ± 0.7	2.8 ± 0.3	1.9 ± 0.1	4.9 ± 0.7	0.2 ± 0.01	0.1 ± 0.003	2.9 ± 0.2
coch-JI2165	21.8 ± 1.2	17.0 ± 1.3	3.9 ± 0.2**	1.8 ± 0.1	4.7 ± 0.5	0.2 ± 0.01	0.07 ± 0.006	3.1 ± 0.2
Parvus	27.5 ± 2.4	14.1 ± 0.9	3.3 ± 0.2	1.8 ± 0.1	5.4 ± 0.8	0.2 ± 0.02	0.09 ± 0.01	2.1 ± 0.1
coch-JI2757	21.0 ± 1.2*	16.9 ± 0.8*	3.5 ± 0.2	1.9 ± 0.1	7.2 ± 0.6	0.3 ± 0.02*	0.11 ± 0.1	2.3 ± 0.9

792

793

794

795

796

797

798

799

800

801

802

803 **Supplemental Table 3. Genotype-specific DEGs across developmental pathways in**
804 **developing and mature nodules (vs WT root primordia)**

805 Pisum sativum genes that are differentially expressed only in WT or only in *coch* (genotype-
806 specific) when comparing developing nodules and mature nodules to WT root primordia.
807 Genes that were differentially expressed in both genotypes within the same tissue, or did not
808 differ between WT and *coch* for that tissue, are excluded. Columns list PsCam transcript ID,
809 Psat v1 gene ID, gene symbol, gene name, and per genotype tissue log2FC and q-value, as
810 defined in Methods.

PsCam ID	Psat v1 ID	Gene symbol	Gene name	q-val & log_2FC (relative to WT root primordia)							
				WT Developing nodule		coch Developing nodule		WT Mature nodule		coch Mature nodule	
				q-val	log_2FC	q-val	log_2FC	q-val	log_2FC	q-val	log_2FC
AUXIN PATHWAY											
PsCam042685	Psat2g033840	LAX1	LIKE-AUX1 1 — auxin influx carrier	4.63E-02	-0.83	9.72E-01	0.04	5.25E-07	-1.72	1.14E-07	-1.79
PsCam034535	Psat3g130520	AUX1/LAX2	LIKE-AUX1 2 — auxin influx carrier	3.13E-03	-1.19	7.50E-01	-0.26	2.87E-06	-1.71	5.45E-07	-1.80
PsCam004662	Psat5g280080	MtARF13	Auxin Response Factor 13	2.43E-02	-0.53	9.16E-01	-0.06	1.81E-02	-0.51	1.43E-01	-0.33
PsCam031281	Psat2g042360	MtARF8	Auxin Response Factor 8	9.67E-03	-0.79	9.54E-01	0.05	1.98E-05	-1.15	1.62E-04	-1.01
PsCam056641	Psat0s2445g0040	MtARF33	Auxin Response Factor 33	8.99E-01	0.06	8.22E-01	0.13	2.66E-01	0.31	1.46E-02	0.59
PsCam034334	Psat1g192000	MtARF6	Auxin Response Factor 6	1.69E-02	-0.67	7.49E-01	-0.17	9.16E-08	-1.27	1.07E-07	-1.25
PsCam004861	Psat6g183360	MtARF4	Auxin Response Factor 4	1.86E-01	-0.48	4.45E-02	-0.70	4.59E-06	-1.23	6.76E-08	-1.41
PsCam056304	Psat6g102800	MtIAA1	Aux/IAA 1 — auxin-responsive transcriptional repressor	1.97E-02	-1.63	8.15E-01	-0.34	1.73E-05	-2.61	7.99E-05	-2.38
PsCam001343	Psat5g297360	MtIAA11	Aux/IAA 11 — auxin-responsive transcriptional repressor	4.51E-02	-1.26	6.97E-01	-0.43	1.84E-04	-2.00	2.03E-06	-2.45

PsCam002187	Psat7g253440	MtIAA14	Aux/IAA 14 — auxin-responsive transcriptional repressor	3.56E-03	-2.58	8.86E-02	-1.84	6.76E-06	-3.61	1.77E-08	-4.38
PsCam006879	Psat2g134720	MtIAA18	Aux/IAA 18 — auxin-responsive transcriptional repressor	4.39E-02	-0.41	8.63E-01	-0.08	1.09E-01	-0.31	7.79E-02	-0.33
PsCam052042	Psat3g061720	MtIAA21	Aux/IAA 21 — auxin-responsive transcriptional repressor	9.95E-03	-2.13	7.33E-02	-1.74	2.74E-04	-2.71	2.57E-09	-4.19
PsCam051472	Psat4g197240	MtIAA23	Aux/IAA 23 — auxin-responsive transcriptional repressor	4.57E-02	-1.87	3.37E-01	-1.21	2.53E-05	-3.31	6.25E-07	-3.80
PsCam050216	Psat7g014720	MtIAA25	Aux/IAA 25 — auxin-responsive transcriptional repressor	3.12E-03	-1.49	9.50E-01	-0.08	2.52E-02	-1.11	2.78E-05	-1.90
PsCam050937	Psat6g057880	MtIAA3	Aux/IAA 3 — auxin-responsive transcriptional repressor	4.36E-03	-2.84	4.96E-01	-1.09	4.08E-05	-3.72	5.86E-07	-4.38
PsCam013177	Psat0s1875g0080	MtIAA4	Aux/IAA 4 — auxin-responsive transcriptional repressor	9.47E-03	-0.84	7.84E-01	0.18	1.01E-05	-1.27	3.13E-03	-0.87
PsCam039815	Psat6g158720	MtIAA6	Aux/IAA 6 — auxin-responsive transcriptional repressor	5.62E-02	1.08	3.04E-01	0.75	2.47E-01	0.64	3.96E-03	1.38
PsCam035994	Psat7g127400	PIN1	PIN-FORMED 1 — auxin efflux carrier	9.06E-01	0.09	8.82E-01	0.13	8.71E-01	-0.08	3.81E-02	-0.75
PsCam020795	Psat3g080160	PIN10	PIN-FORMED 10 — auxin efflux carrier	4.40E-01	-0.40	9.82E-01	-0.02	1.08E-02	-0.91	1.81E-01	-0.51
PsCam048287	Psat1g032680	PIN4.2	PIN-FORMED 4.2 — auxin efflux carrier	3.36E-01	-0.36	9.47E-01	-0.05	4.05E-02	-0.57	6.34E-01	-0.16
PsCam059406	Psat0s502g0040	PIN6	PIN-FORMED 6 — auxin efflux carrier	9.63E-01	0.08	1.82E-01	1.35	2.80E-01	-0.91	6.97E-03	-1.95
PsCam017219	Psat2g093920	TAA-2	TRYPTOPHAN AMINOTRANSFERASE OF ARABIDOPSIS 2	5.43E-04	-2.64	2.12E-01	-1.32	3.35E-04	-2.62	7.79E-04	-2.42
PsCam038488	Psat3g024760	YUC10	YUCCA10 — flavin mono-oxygenase involved in auxin biosynthesis	3.35E-03	-2.05	6.43E-01	-0.58	3.69E-06	-2.92	2.33E-10	-3.85
PsCam036661	Psat6g167560	TIR1.1	TRANSPORT INHIBITOR RESPONSE 1.1	2.12E-02	0.58	7.49E-01	-0.15	4.36E-05	0.89	9.18E-06	0.94
CYTOKININ PATHWAY											

PsCam038941	Psat6g060960	IPT3	ISOPENTENYL TRANSFERASE 3	4.48E-02	1.15	5.86E-01	0.50	7.35E-03	1.36	1.55E-02	1.22
PsCam037932	Psat1g075000	MtCYP735A10	CYTOCHROME P450 MONOOXYGENASE 735A10	5.88E-06	2.64	2.79E-01	0.96	9.49E-04	1.94	2.10E-03	1.79
PsCam031214	Psat6g071200	MtLOG2	LONELY GUY 2	1.64E-07	2.73	6.91E-02	1.26	2.00E-07	2.67	8.34E-07	2.51
PsCam039655	Psat6g084480	MtLOG5	LONELY GUY 5	6.03E-01	-0.28	1.10E-03	-1.16	1.25E-03	-1.05	1.38E-04	-1.20
PsCam011148	Psat4g015840	MtCKX8 2	CYTOKININ OXIDASE/DEHYDROGENASE 8-2	2.05E-02	2.05	4.70E-01	0.97	6.17E-02	1.58	1.47E-02	1.95
PsCam033636	Psat5g097280	CHK3	CYTOKININ RECEPTOR HISTIDINE KINASE 3	3.69E-02	-0.62	7.75E-02	-0.59	7.69E-08	-1.32	1.21E-08	-1.38
PsCam031202	Psat4g192080	MtRRA11	TYPE-A RESPONSE REGULATOR 11	5.74E-03	2.77	6.55E-01	0.81	1.31E-03	2.99	1.64E-04	3.39
PsCam002032	Psat0s644g0040	MtRRA4	TYPE-A RESPONSE REGULATOR 4	6.64E-02	-0.61	2.02E-02	-0.78	1.77E-03	-0.89	2.19E-05	-1.15
PsCam049006	Psat4g007520	MtRRB16	TYPE-B RESPONSE REGULATOR 16	4.35E-02	-0.40	3.61E-01	-0.25	1.95E-01	-0.25	1.67E-01	-0.26
PsCam045578	Psat6g027120	MtRRB21	TYPE-B RESPONSE REGULATOR 21	4.94E-06	-1.14	2.70E-01	-0.42	5.75E-08	-1.31	4.89E-08	-1.30
PsCam004652	Psat4g078200	MtRRB24	TYPE-B RESPONSE REGULATOR 24	3.67E-01	1.54	2.97E-01	1.88	8.53E-03	3.20	6.52E-02	2.30
PsCam043337	Psat5g128280	MtRRB3	TYPE-B RESPONSE REGULATOR 3	4.82E-01	0.36	5.97E-01	-0.33	7.66E-01	-0.14	7.91E-03	-0.88
GIBBERELLIN PATHWAY											
PsCam042984	Psat1g164440	KAO1	ent-kaurenoic acid oxidase 1	2.27E-02	-1.03	1.81E-01	-0.75	4.56E-04	-1.39	5.27E-05	-1.56
PsCam000417	Psat5g070280	GA13OX1	GA 13 Oxidase 1	1.84E-01	0.85	2.19E-01	-0.88	6.95E-02	0.97	4.55E-02	1.03
PsCam037814	Psat1g127560	GA13OX2	GA 13 Oxidase 2	2.78E-03	-2.15	1.46E-02	-1.94	7.21E-02	-1.31	1.75E-03	-2.08
PsCam054835	Psat1g113960	GA20OX2	GA 20 Oxidase 2	4.11E-07	4.14	1.50E-01	1.66	1.24E-06	3.92	2.07E-06	3.78

PsCam000885	Psat4g196400	GA20OX3	GA 20 Oxidase 3	6.85E-01	-0.85	6.34E-01	1.09	6.11E-02	-2.39	1.50E-03	-3.72
PsCam038799	Psat0s2303g0120	GA20OX6	GA 20 Oxidase 6	2.51E-02	2.82	6.42E-01	1.00	9.61E-04	3.67	2.99E-04	3.91
PsCam023497	Psat7g174680	GA20ox10	GIBERELLIC ACID 20-OXIDASE	3.38E-01	-1.16	3.20E-01	-1.31	7.20E-02	-1.65	1.84E-03	-2.62
PsCam039180	Psat0s1953g0280	GA2OX4	GA 2-oxidase 4	5.08E-03	1.55	2.22E-03	1.74	8.56E-02	0.96	2.57E-02	1.17
PsCam037091	Psat4g224560	GA2OC8	GA 2-oxidase 8	4.23E-06	3.50	5.37E-02	1.87	2.78E-09	4.31	2.54E-11	4.76
PsCam039132	Psat5g157800	GAOL-15	GIBBERELLIN GA2 OXIDASE-LIKE 15	8.62E-05	1.68	2.97E-01	0.67	2.22E-06	1.93	1.34E-10	2.53
NODULATION PATHWAY											
PsCam034334	Psat1g192000	ARF6	Auxin Response Factor 6	1.69E-02	-0.67	7.49E-01	-0.17	9.16E-08	-1.27	1.07E-07	-1.25
PsCam031281	Psat2g042360	ARF8	Auxin Response Factor 8	9.67E-03	-0.79	9.54E-01	0.05	1.98E-05	-1.15	1.62E-04	-1.01
PsCam034535	Psat3g130520	AUX1/LAX2	LIKE-AUX1 2 — auxin influx carrier	3.13E-03	-1.19	7.50E-01	-0.26	2.87E-06	-1.71	5.45E-07	-1.80
PsCam048287	Psat1g032680	PIN4.2	PIN-FORMED 4.2 — auxin efflux carrier	3.36E-01	-0.36	9.47E-01	-0.05	4.05E-02	-0.57	6.34E-01	-0.16
PsCam035994	Psat7g127400	PIN1	PIN-FORMED 1 — auxin efflux carrier	9.06E-01	0.09	8.82E-01	0.13	8.71E-01	-0.08	3.81E-02	-0.75
PsCam056304	Psat6g102800	IAA1	Aux/IAA 1 — auxin-responsive transcriptional repressor	1.97E-02	-1.63	8.15E-01	-0.34	1.73E-05	-2.61	7.99E-05	-2.38
PsCam036661	Psat6g167560	TIR1.1	TRANSPORT INHIBITOR RESPONSE 1.1	2.12E-02	0.58	7.49E-01	-0.15	4.36E-05	0.89	9.18E-06	0.94
PsCam055886	Psat6g115840	CCS52B.1	CELL CYCLE SWITCH 52 B.1	7.45E-05	0.77	8.21E-01	0.10	1.11E-06	0.90	4.51E-11	1.17
PsCam036060	Psat3g198920	CDKC	CYCLIN-DEPENDENT KINASE C	8.91E-04	1.49	3.90E-01	0.60	2.50E-05	1.77	6.54E-06	1.85
PsCam057520	Psat5g085560	CYCA1	CYCLIN A1	1.89E-02	-0.63	3.12E-01	-0.37	1.50E-05	-1.01	2.53E-07	-1.17

PsCam052387	Psat2g137440	H3K27	Histone H3	7.95E-01	-0.31	2.97E-01	-0.97	1.86E-01	-0.92	1.01E-03	-1.98
PsCam006855	Psat4g145000	RBR1	RETINOBLASTOMA-RELATED 1	8.01E-01	0.09	9.76E-01	0.02	1.56E-01	0.28	2.82E-02	0.39
PsCam045630	Psat4g124480	PG	POLYGALACTURONASE	1.63E-02	2.33	9.72E-01	0.10	8.50E-04	2.90	3.40E-02	1.91
PsCam005001		XTH23	Xyloglucan endotransglucosylase/hydrolase 23	6.42E-06	-4.21	4.99E-01	-1.10	1.83E-05	-3.93	3.21E-03	-2.76
PsCam046602		XTH22	Xyloglucan endotransglucosylase/hydrolase 22	8.46E-01	0.24	8.28E-01	0.32	1.42E-01	-1.01	4.52E-02	-1.29
PsCam056516	Psat2g167760	H3K27	HISTONE-LYSINE N-METHYLTRANSFERASE	1.33E-01	0.42	9.91E-01	-0.01	3.33E-01	0.26	1.90E-02	0.54
PsCam050229	Psat2g177440	ATHB2	HOMEOBOX PROTEIN 2 (HD-ZIP II family).	4.64E-02	-0.66	4.78E-01	-0.34	2.97E-05	-1.16	1.54E-03	-0.88
PsCam042232	Psat5g045920	GRF6	GROWTH-REGULATING FACTOR 6	9.65E-01	0.02	1.24E-01	-0.41	2.41E-01	0.27	2.28E-02	0.46
PsCam034697	Psat1g133440	GRF-LIKE5	GRF-like transcription factor 5	3.07E-02	-2.63	1.75E-01	-2.03	2.68E-02	-2.48	9.34E-02	-1.90
PsCam023316	Psat2g181200	KNOX4	KNOTTED1-LIKE HOMEOBOX 4	3.32E-02	-1.51	7.09E-01	-0.48	1.68E-05	-2.58	3.84E-06	-2.71
PsCam054829	Psat5g030920	KNOX5	KNOTTED1-LIKE HOMEOBOX 5	2.07E-01	0.47	5.76E-03	0.90	3.20E-03	0.86	3.20E-04	1.01
PsCam045688	Psat0s1183g0080	KNOX8	KNOTTED1-LIKE HOMEOBOX 8	1.81E-01	-1.12	9.63E-01	-0.09	5.32E-02	-1.35	2.90E-10	-3.82
PsCam036983	Psat6g123400	PLT3	PLETHORA 3	2.57E-02	1.05	6.75E-01	0.35	5.05E-01	0.35	1.36E-01	0.67
PsCam050296	Psat4g013080	PLT5	PLETHORA 5	7.11E-01	0.25	7.95E-01	0.22	9.48E-01	-0.04	4.02E-02	-0.79
PsCam039770	Psat5g277280	LBD11.2	LOB DOMAIN-CONTAINING PROTEIN 11	1.75E-02	1.85	4.49E-02	1.75	1.98E-02	1.69	1.58E-01	1.07
PsCam016769	Psat7g224320	RC7	Root Cap 7	1.22E-01	-3.32	4.63E-01	-2.15	2.24E-01	-2.41	1.49E-02	-4.28

PsCam011218	Psat5g246320	RC6	Root Cap 6	2.96E-01	-2.53	8.30E-01	-0.90	4.64E-01	-1.59	4.45E-02	-3.67
PsCam055031	Psat2g045000	TMK1/4	Transmembrane Kinase	9.61E-01	0.04	6.50E-01	-0.29	7.86E-01	0.13	3.78E-02	0.71
PsCam038971	Psat2g042200	RHD6	ROOT HAIR DEFECTIVE 6	2.12E-03	-2.99	8.37E-02	-2.07	3.73E-03	-2.71	3.20E-04	-3.22
PsCam049996	Psat7g100600	NPH3	NON-PHOTOTROPIC HYPOCOTYL 3	3.84E-03	-1.29	1.22E-01	-0.87	7.83E-05	-1.61	1.25E-03	-1.32
PsCam048824	Psat5g067040	BRI1	BRASSINOSTEROID INSENSITIVE 1	3.10E-01	-0.24	3.64E-02	-0.43	1.68E-01	-0.26	4.55E-02	-0.35
PsCam009542	Psat0s2056g0040	BRUSH	BRUSH	5.29E-01	-0.79	9.49E-01	-0.15	3.30E-01	-0.92	2.12E-02	-1.88
PsCam037392	Psat0s5923g0040	CHIT5	CHITINASE 5	6.09E-04	1.16	8.46E-01	0.15	6.66E-04	1.11	1.77E-05	1.34
PsCam036593	Psat6g071760	CNGC15a	CYCLIC NUCLEOTIDE GATED CHANNELS 15A	3.05E-01	0.89	1.77E-02	1.76	9.90E-01	-0.01	1.97E-01	-0.89
PsCam049032	Psat1g222280	DMI1	DOES NOT MAKE Infections 1	4.64E-02	0.79	4.94E-01	0.40	9.15E-05	1.31	4.17E-06	1.50
PsCam045655	Psat4g141880	CCaMK/DMI3	CALCIUM CALMODULIN KINASE ,DOES NOT MAKE Infections 3	1.38E-04	0.95	1.30E-01	0.50	5.49E-08	1.27	5.44E-13	1.63
PsCam034075	Psat3g159880	FNSII	FLAVONE SYNTHASE	2.76E-03	-0.92	1.96E-01	-0.53	4.40E-08	-1.50	1.73E-06	-1.31
PsCam000836	Psat1g124400	NENA	NENA	3.93E-02	0.47	8.79E-01	-0.08	7.36E-05	0.77	1.72E-04	0.72
PsCam035737	Psat0s741g0280	NSP1	NODULATION SIGNALING PATHWAY 1	2.96E-02	0.69	2.86E-01	0.45	1.62E-01	0.43	2.00E-02	0.66
PsCam037255	Psat5g133360	NSP2	NODULATION SIGNALING PATHWAY 2	3.39E-02	-1.01	2.73E-01	-0.69	9.57E-07	-1.97	1.04E-06	-1.93
PsCam050140	Psat5g008600	SIP1	SYMRK INTERACTING PROTEIN 1	1.64E-02	1.40	5.36E-01	0.57	2.57E-05	2.15	8.99E-07	2.44
PsCam004861	Psat6g183360	ARF4/ARF16a	AUXIN RESPONSE FACTOR 16a	1.86E-01	-0.48	4.45E-02	-0.70	4.59E-06	-1.23	6.76E-08	-1.41

PsCam016955	Psat4g140120	EIN2a	ETHYLENE INSENSITIVE 2	3.36E-01	-0.44	7.86E-01	-0.20	1.20E-01	-0.56	2.92E-02	-0.73
PsCam023497	Psat7g174680	GA20ox10	GIBERELLIC ACID 20-OXIDASE	3.38E-01	-1.16	3.20E-01	-1.31	7.20E-02	-1.65	1.84E-03	-2.62
PsCam005627	Psat4g095600	LAN	LACK OF SYMBIONT ACCOMMODATIONÂ	6.85E-02	1.05	3.71E-02	1.25	1.39E-01	0.80	4.05E-02	1.03
PsCam048664	Psat2g010560	N5	NODULIN 5	5.57E-06	1.76	9.81E-02	0.86	4.32E-08	2.05	7.16E-09	2.13
PsCam034822	Psat5g092760	NPL	NODULE PECTATE LYASE	2.89E-02	3.42	5.64E-01	1.44	5.21E-03	3.91	8.66E-03	3.63
PsCam055889	Psat5g026680	Rboh	Rboh(NADPH-oxidase)	2.73E-02	-1.47	7.34E-02	-1.35	6.49E-03	-1.63	1.42E-05	-2.43
PsCam017590	Psat1g123800	RFG1	RESISTANCE GENE ANALOGUE	7.13E-01	-0.35	7.42E-01	0.37	6.30E-01	-0.34	3.05E-02	-1.18
PsCam009798	Psat4g191080	ANN 1.1	ANNEXIN1	1.33E-05	1.41	7.99E-01	0.19	1.02E-08	1.76	2.31E-08	1.71
PsCam043064	Psat4g147120	ANN 1.2	ANNEXIN1	6.86E-05	2.49	5.97E-01	0.61	1.22E-07	3.13	1.39E-07	3.08
PsCam031281	Psat2g042360	ARF8	AUXIN RESPONSE FACTOR 8	9.67E-03	-0.79	9.54E-01	0.05	1.98E-05	-1.15	1.62E-04	-1.01
PsCam037340	Psat0s1712g0040	BG2	?-1,3 -GLUCANASE	2.17E-01	-0.68	9.02E-01	-0.13	6.97E-02	-0.81	1.07E-03	-1.33
PsCam042733	Psat3g108760	BPS1	BYPASS1	5.04E-07	1.36	6.56E-01	0.24	2.24E-10	1.66	1.07E-08	1.49
PsCam055886	Psat0s3705g0040	CCS 52a	CELL CYCLE SWITCH GENE encoding a 52 kDa protein	7.45E-05	0.77	8.21E-01	0.10	1.11E-06	0.90	4.51E-11	1.17
PsCam038941	Psat6g060960	IPT3	ISOPENTENYL TRANSFERASE	4.48E-02	1.15	5.86E-01	0.50	7.35E-03	1.36	1.55E-02	1.22
PsCam042941	Psat6g028400	KNOX3	KNOX3	4.84E-08	1.95	6.62E-02	0.87	1.95E-13	2.52	4.82E-15	2.66
PsCam054829	Psat5g030920	KNOX5	KNOX5	2.07E-01	0.47	5.76E-03	0.90	3.20E-03	0.86	3.20E-04	1.01
PsCam034535	Psat3g130520	LAX2	LIKE-AUX1 1 — auxin influx carrier	3.13E-03	-1.19	7.50E-01	-0.26	2.87E-06	-1.71	5.45E-07	-1.80

PsCam030891	Psat0s1505g0120	LIN	LUMPY InfectionS	1.33E-03	0.65	4.38E-01	0.25	5.14E-02	0.40	1.34E-02	0.48
PsCam053713	Psat3g010480	NY-YC1	NUCLEAR FACTOR YC1	1.08E-03	0.61	7.35E-01	0.13	1.00E-06	0.83	5.97E-08	0.90
PsCam035382	Psat5g295880	PEN3-like	PENETRATION3 - LIKE	3.43E-03	-1.05	4.44E-01	-0.43	1.69E-06	-1.55	2.47E-08	-1.76
PsCam036983	Psat2g089880	PLT3	PLETHORA 3	2.57E-02	1.05	6.75E-01	0.35	5.05E-01	0.35	1.36E-01	0.67
PsCam001796	Psat7g071680	SGF14	Soybean G-BOX FACTOR 14-3-3	5.13E-02	-0.40	2.35E-03	-0.60	9.18E-03	-0.47	1.57E-01	-0.27
PsCam042487	Psat5g091280	CRA2	COMPACT ROOT ARCHITECTURE 2	4.62E-02	-0.82	8.13E-01	-0.20	6.69E-02	-0.70	1.86E-03	-1.09
PsCam042402	Psat1g068760	KLV1	KLAVIER 1	7.12E-01	0.12	2.98E-02	0.47	3.54E-01	0.20	3.58E-01	0.19
PsCam016891	Psat1g032360	KLV2	KLAVIER 2	6.14E-01	0.18	2.91E-02	0.57	3.40E-01	0.25	1.98E-01	0.31
PsCam042790	Psat7g221800	NNC1	NODULE NUMBER CONTROL 1	9.76E-01	-0.04	5.98E-01	-0.60	1.25E-01	-1.03	4.75E-02	-1.26
PsCam037480	Psat1g087960	TML2	TOO MUCH LOVE 2	5.55E-01	0.48	2.09E-01	-0.92	8.80E-04	1.69	6.27E-01	0.31
PsCam051909	Psat5g204840	DNF1	DEFECTIVE IN Nitrogen Fixation1	2.75E-10	1.43	5.93E-02	0.57	2.42E-12	1.56	6.23E-10	1.38
PsCam009630	Psat6g003240	SYT	SYNAPTOGAMIN	7.38E-01	-0.10	4.25E-02	-0.43	8.33E-01	0.05	4.98E-01	0.14
PsCam001433	Psat1g170080	VAMP721d	VESICLE ASSOCIATED MEMBRANE PROTEIN	7.28E-04	0.68	2.15E-01	0.34	2.53E-05	0.79	1.90E-08	1.02
PsCam000259	Psat5g207560	MATE1.1	MULTIDRUG AND TOXIC COMPOUND EXTRUSION 1	1.13E-03	-0.78	8.29E-01	-0.12	6.01E-03	-0.64	6.84E-02	-0.44
PsCam045540	Psat4g191600	MATE1.2	MULTIDRUG AND TOXIC COMPOUND EXTRUSION 1	4.16E-03	2.04	4.65E-01	0.82	5.18E-05	2.63	3.95E-06	2.91
PsCam000872	Psat7g211200	MTP2	METAL TOLERANCE PROTEIN 2	2.15E-02	0.63	9.26E-01	-0.06	7.92E-02	0.46	4.48E-02	0.51
PsCam036634	Psat5g003760	PRAT3	GLUTAMINE PHOSPHORIBOSYL	3.98E-02	-1.53	7.28E-01	-0.47	2.12E-04	-2.35	1.57E-05	-2.66

			PYROPHOSPHATE AMIDOTRANSFERASE 3								
PsCam012944	Psat3g057880	PT5	PHOSPHATE TRANSPORTER 5	5.78E-01	-1.05	5.90E-01	1.15	1.24E-01	-1.97	3.04E-02	-2.58
PsCam016924	Psat6g125640	PT7	PHOSPHATE TRANSPORTER 7	9.19E-01	-0.27	5.63E-01	-1.28	6.75E-03	-3.39	6.65E-01	0.68
PsCam045132	Psat4g019440	SUS1	SUCROSE SYNTHASE 1	7.18E-05	1.80	5.04E-01	0.52	4.95E-08	2.32	3.24E-10	2.62
PsCam044001	Psat1g139760	SUS3	SUCROSE SYNTHASE 3	7.71E-01	-0.49	8.82E-01	0.34	1.75E-01	-1.36	1.23E-02	-2.26
PsCam046623	Psat2g130320	UPS1-1	UREIDE PERMEASE	1.41E-02	-1.24	9.55E-01	-0.08	1.47E-03	-1.46	1.02E-04	-1.71
PsCam007366	Psat1g038720	CAS31	COLD ACCLIMATION SPECIFIC	2.41E-02	-2.10	1.06E-01	-1.77	5.47E-04	-2.83	2.73E-08	-4.29
PsCam028901	Psat0s4087g0080	CP6	CYSTEINE PROTEINASE 6	4.70E-02	4.40	9.05E-02	4.23	3.71E-01	2.04	4.53E-02	3.97
PsCam004978	Psat6g018800	VPE	VACUOLAR PROCESSING ENZYME	1.23E-06	-1.01	1.16E-01	-0.45	7.60E-04	-0.72	1.32E-11	-1.34
PsCam038402	Psat6g125480	ERF1	ETHYLENE RESPONSE FACTOR 1	2.49E-01	-0.73	6.27E-01	-0.44	2.26E-02	-1.12	6.74E-02	-0.91
PsCam036127	Psat1g095400	ERN2	ETHYLENE RESPONSE FACTOR REQUIRED FOR NODULATION2	3.27E-02	-1.27	9.20E-01	0.14	4.47E-05	-2.08	1.25E-06	-2.39
PsCam012963	Psat3g090960	GS52	Glycine sojae 52	1.95E-01	0.55	9.47E-01	0.06	1.43E-01	-0.53	3.40E-02	-0.71
PsCam006801	Psat6g037200	GS	GLUTAMINE SYNTHETASE ,NADH-dependent GLUTAMATE SYNTHASE	8.47E-05	1.53	8.01E-01	0.22	1.58E-07	1.93	8.89E-08	1.94

811

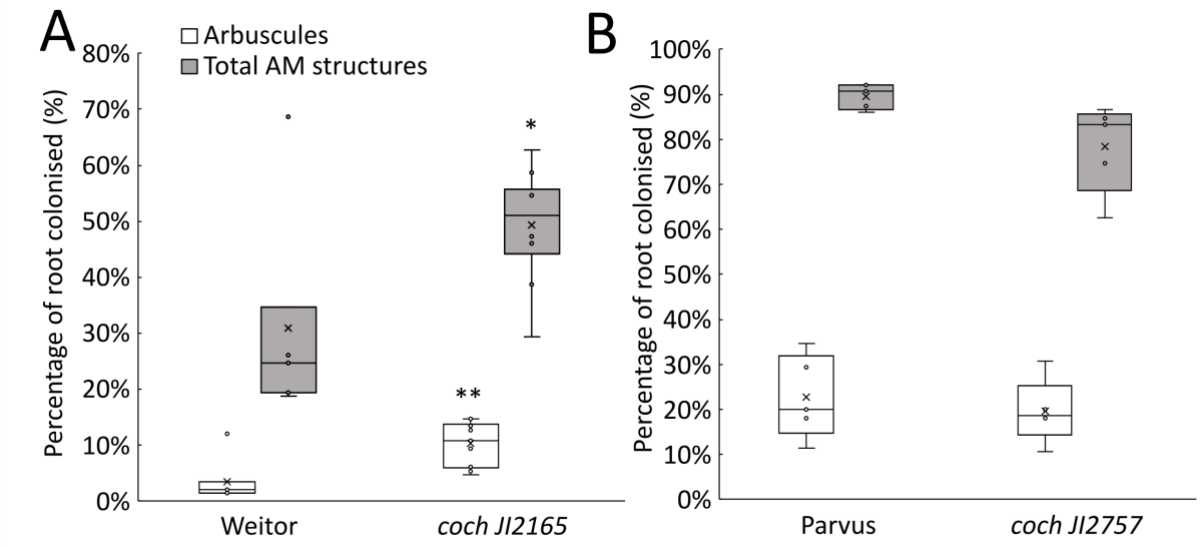

Supplementary Figure 1. Mycorrhizal phenotypes *coch*-JI2165 and *coch*-JI2757 mutants and their corresponding isogenic wild-type lines, Weitor and Parvus.

(A-B) Percentage of roots colonised with arbuscules or total arbuscular mychorrizal (AM) structures (arbuscules, vesicles and hyphae) in *coch-JI2165* and wild type Weitor (A) and *coch-JI2757* and wild type Parvus (B). Data are shown as box plots: boxes represent the interquartile range, horizontal lines show the median, and whiskers indicate the full data range. $n = 7–10$; $p < 0.05$ (*), $p < 0.01$ (**), Student's *t*-test.

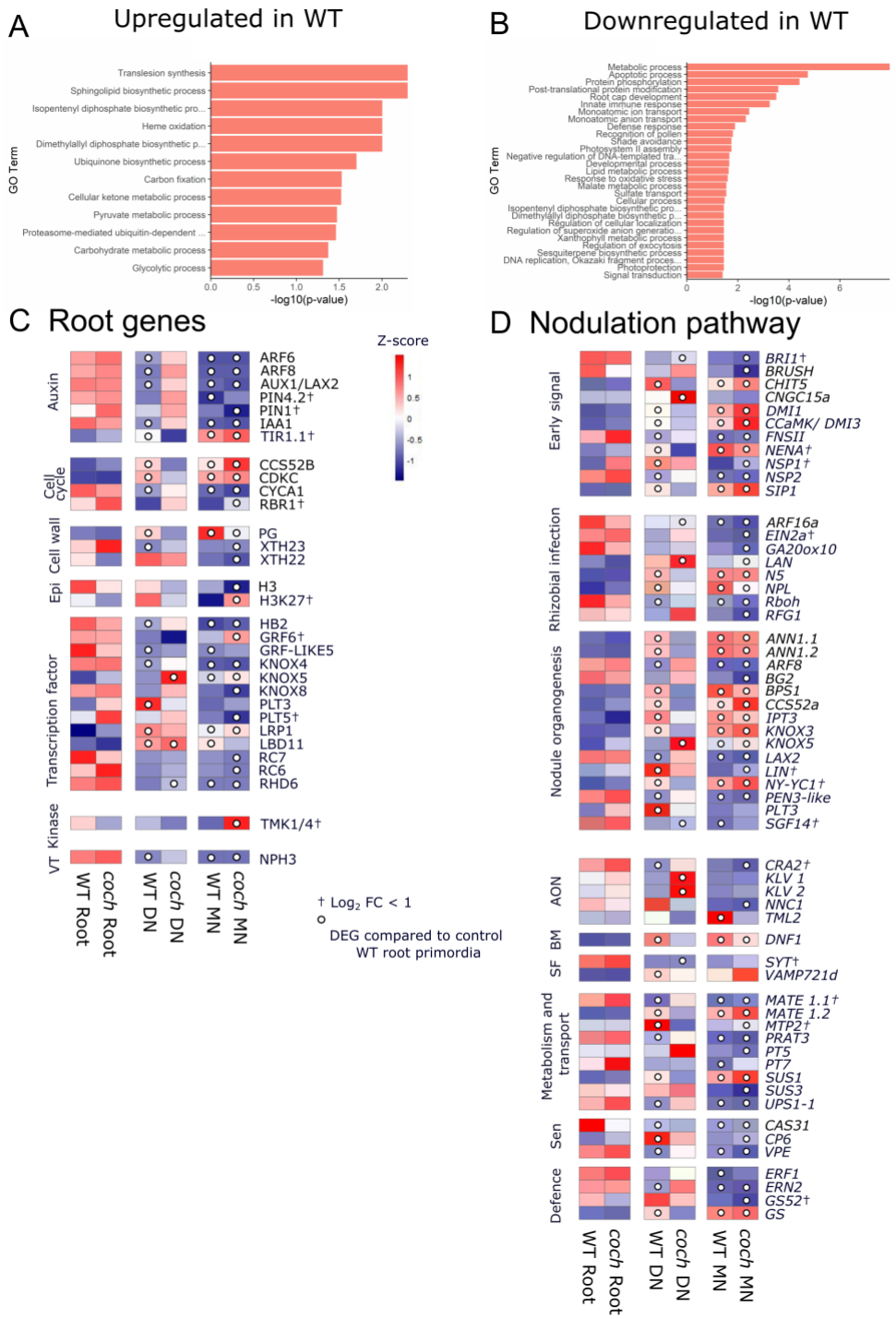

Supplementary Figure 2. Gene ontology enrichment and expression profiles of root and nodulation-related genes

(A–B) Gene Ontology (GO) enrichment analysis of genes uniquely upregulated (A) or downregulated (B) in wild-type plants in developing and mature nodules, which showed no response in *coch* mutants.

(C–D) Heatmaps showing the expression of genes involved in lateral root formation (C) and nodulation (D) that were differentially expressed between wild-type and *coch* mutants in either developing or mature nodules. The heatmap colour scale represents Z-scores of normalized gene expression. White circles within each heatmap cell indicate that the gene in that specific condition was significantly differentially expressed relative to the wild-type root primordia (q-value < 0.05). Genes marked with a cross (†) indicate that although differentially expressed, their absolute $\log_2$ fold change ($\log_2$FC) was < 1.

Samples were collected from 6-week-old plants, 4 weeks post-inoculation with *Rhizobium*. Tissues included root tips, developing nodules, and mature nodules for wild-type, and abnormal nodules for *coch* mutants.

Abbreviations: Epi – Epigenetics, VT – Vesicular transport, AON – Autoregulation of nodulation, BM – Bacterial maturation, SF – Symbiosome formation, Sen – Senescence. DN: Developing nodule. MN: Mature nodule. Gene symbols and full names are listed in Table S3.

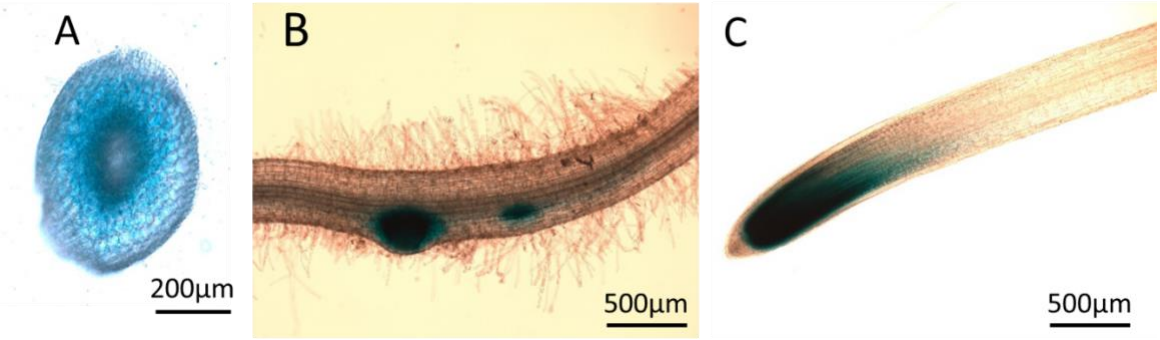

Supplementary Figure 3. Tissue-specific expression of the *CO2* promoter in pea (*Pisum sativum*) used in Figure 4.

Hairy root-transformed *Pisum sativum* (cv. Torsdag) plants were used to analyse *CO2* promoter activity using a *CO2::GUS* construct (β-glucuronidase reporter gene). GUS activity is indicated by blue staining.

(A) Cross-section of a root showing *CO2*::*GUS* expression in the cortex at the basal meristematic zone and above.

(B) *CO2*::*GUS* expression in early nodule primordia.

(C) *CO2*::*GUS* activity in the root tip.

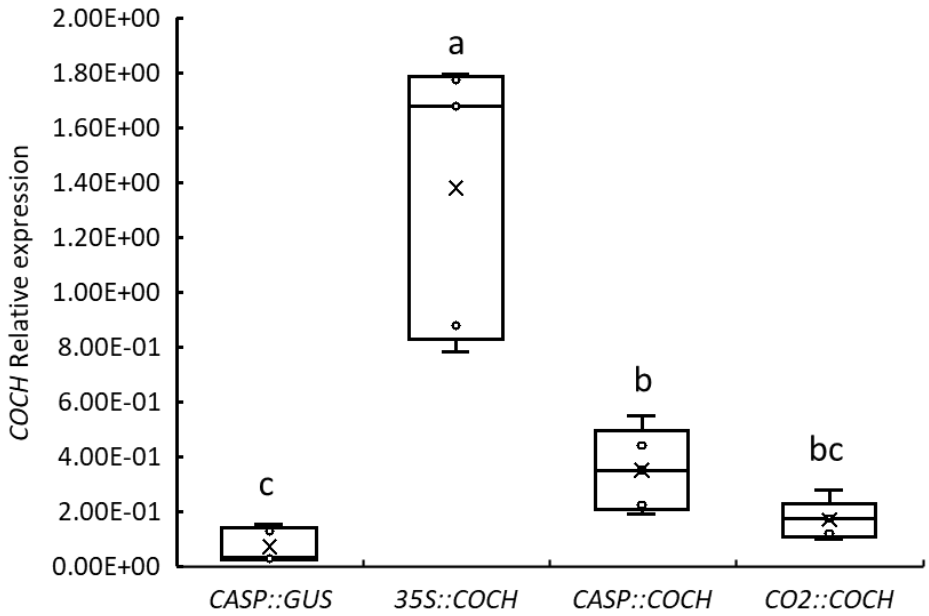

858

859 **Supplementary Figure 4. Relative expression of *PsCOCH* in ectopic expression hairy root**
860 **transformation experiment shown in Figure 4.**

861 Relative expression of *PsCOCH* in transformed pea hairy roots expressing different constructs
862 (*CASP::GUS, 35S::COCH, CASP::COCH, CO2::COCH*). Expression was normalized to the
863 geometric mean of two housekeeping genes: *TFIIa* and *Actin*. Whole transformed roots were
864 harvested 3 weeks post-inoculation with *Rhizobium leguminosarum* for RNA extraction and
865 qPCR. Data are shown as box plots**:** boxes represent the interquartile range, horizontal lines
866 show the median, and whiskers indicate the full data range. n = 5. Different letters indicate
867 statistically significant differences between constructs as determined by one-way ANOVA
868 followed by Tukey's HSD post hoc test ($p < 0.05$).

869

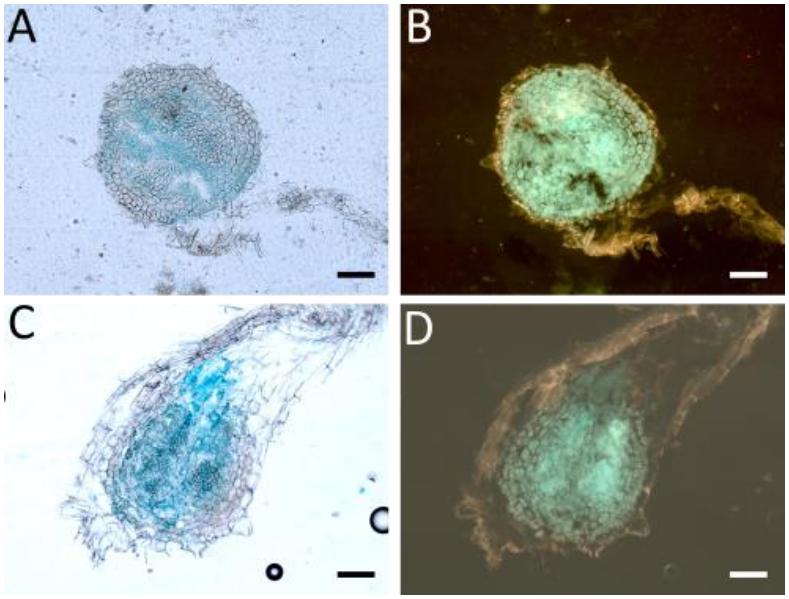

Supplemental Figure 5. *DR5::GUS* staining pattern seen throughout *coch* mature nodules shown in Figure 6H.

Transverse sections of *coch* mutant nodules showing DR5::GUS activity. (A–B) Top region and (C–D) basal region of the nodule. Panels (B) and (D) show GFP-tagged rhizobia. Scale bar = 100 µm.

877 **REFERENCES**

878 **Aida, M., Beis, D., Heidstra, R., Willemsen, V., Blilou, I., Galinha, C., Nussaume, L., Noh, Y.-S.,**
879 **Amasino, R., and Scheres, B.** (2004). The *PLETHORA* genes mediate patterning of the *Arabidopsis*
880 root stem cell niche. Cell **119**:109-120.
881 **Alexa, A., Rahnenführer, J., and Lengauer, T.** (2006). Improved scoring of functional groups from
882 gene expression data by decorrelating GO graph structure. Bioinformatics **22**:1600-1607.
883 10.1093/bioinformatics/btl140.
884 **Alves-Carvalho, S., Aubert, G., Carrere, S., Cruaud, C., Brochot, A.L., Jacquin, F., Klein, A., Martin,**
885 **C., Boucherot, K., and Kreplak, J.** (2015). Full-length de novo assembly of RNA-seq data in pea
886 (*Pisum sativum* L.) provides a gene expression atlas and gives insights into root nodulation in this
887 species. The Plant Journal **84**:1-19.
888 Andrews, S. (2017). FastQC: a quality control tool for high throughput sequence data. 2010.
889 **Ariel, F., Brault-Hernandez, M., Laffont, C., Huault, E., Brault, M., Plet, J., Moison, M., Blanchet, S.,**
890 **Ichanté, J.L., and Chabaud, M.** (2012). Two direct targets of cytokinin signaling regulate symbiotic
891 nodulation in *Medicago truncatula*. The Plant Cell **24**:3838-3852.
892 **Azarakhsh, M., and Lebedeva, M.A.** (2023). Lateral Root versus Nodule: The Auxin-Cytokinin
893 Interplay. Journal of Plant Growth Regulation **42**:6903-6919. 10.1007/s00344-023-10983-4.
894 **Bielach, A., Podlesáková, K., Marhavy, P., Duclercq, J., Cuesta, C., Müller, B., Grunewald, W.,**
895 **Tarkowski, P., and Benková, E.** (2012). Spatiotemporal regulation of lateral root organogenesis in
896 *Arabidopsis* by cytokinin. Plant Cell **24**:3967-3981. 10.1105/tpc.112.103044.
897 **Blixt, S.** (1967). Linkage studies in *Pisum*. VII. The manifestation of the genes *cri* and *coch* and the
898 double-recessive in *Pisum*.
899 **Boivin, S., Kazmierczak, T., Brault, M., Wen, J., Gamas, P., Mysore, K.S., and Frugier, F.** (2016).
900 Different cytokinin histidine kinase receptors regulate nodule initiation as well as later nodule
901 developmental stages in *Medicago truncatula*. Plant, cell & environment **39**:2198-2209.
902 **Bolger, A., and Giorgi, F.** (2014). Trimmomatic: A flexible read trimming tool for Illumina NGS data.
903 Bioinformatics **30**:2114-2120.
904 **Bound, S.A., Foo, E., Gélinas-Marion, A., Nichols, D.S., and Nissen, R.** (2022). The impact of
905 dormancy breakers on hormone profiles, fruit growth and quality in sweet cherry. Agriculture
906 **12**:270.
907 **Bray, N.L., Pimentel, H., Melsted, P., and Pachter, L.** (2016). Near-optimal probabilistic RNA-seq
908 quantification. Nature biotechnology **34**:525-527.
909 **Casimiro, I., Marchant, A., Bhalerao, R.P., Beeckman, T., Dhooge, S., Swarup, R., Graham, N., Inzé,**
910 **D., Sandberg, G., and Casero, P.J.** (2001). Auxin transport promotes *Arabidopsis* lateral root
911 initiation. The Plant Cell **13**:843-852.
912 **Cheng, H.-P., and Walker, G.C.** (1998). Succinoglycan is required for initiation and elongation of
913 infection threads during nodulation of alfalfa by *Rhizobium meliloti*. Journal of bacteriology
914 **180**:5183-5191.
915 **Chuck, G., Lincoln, C., and Hake, S.** (1996). *KNAT1* induces lobed leaves with ectopic meristems
916 when overexpressed in *Arabidopsis*. The Plant Cell **8**:1277-1289. 10.1105/tpc.8.8.1277.
917 **Couzigou, J.M., Zhukov, V., Mondy, S., Abu el Heba, G., Cosson, V., Ellis, T.H., Ambrose, M., Wen,**
918 **J., Tadege, M., Tikhonovich, I., et al.** (2012). *NODULE ROOT* and *COCHLEATA* maintain nodule
919 development and are legume orthologs of *Arabidopsis BLADE-ON-PETIOLE* genes. Plant Cell **24**:4498-
920 4510. 10.1105/tpc.112.103747.
921 **Davidson, S.E., Elliott, R.C., Helliwell, C.A., Poole, A.T., and Reid, J.B.** (2003). The pea gene *NA*
922 encodes ent-kaurenoic acid oxidase. Plant Physiology **131**:335-344.
923 **Day, D.A., Lambers, H., Bateman, J., Carroll, B.J., and Gresshoff, P.M.** (1986). Growth comparisons
924 of a supernodulating soybean (*Glycine max*) mutant and its wild-type parent. Physiologia plantarum
925 **68**:375-382.

Dean, G., Casson, S., and Lindsey, K. (2004). *KNAT6* gene of *Arabidopsis* is expressed in roots and is required for correct lateral root formation. Plant Molecular Biology **54**:71-84.

Drapek, C., Rizza, A., Mohd-Radzman, N.A., Schiessl, K., Dos Santos Barbosa, F., Wen, J., Oldroyd, G.E., and Jones, A.M. (2024). Gibberellin dynamics governing nodulation revealed using GIBBERELLIN PERCEPTION SENSOR 2 in *Medicago truncatula* lateral organs. The Plant Cell **36**:4442-4456.

Du, Y., and Scheres, B. (2017). PLETHORA transcription factors orchestrate de novo organ patterning during *Arabidopsis* lateral root outgrowth. Proceedings of the National Academy of Sciences **114**:11709-11714.

Duc, G., and Messager, A. (1989). Mutagenesis of pea (*Pisum sativum L.*) and the isolation of mutants for nodulation and nitrogen fixation. Plant Science **60**:207-213.

Ferguson, B.J., and Reid, J.B. (2005). Cochleata: getting to the root of legume nodules. Plant Cell Physiol **46**:1583-1589. 10.1093/pcp/pci171.

Foo, E., and Davies, N.W. (2011). Strigolactones promote nodulation in pea. Planta **234**:1073-1081. 10.1007/s00425-011-1516-7.

Foo, E., Yoneyama, K., Hugill, C.J., Quittenden, L.J., and Reid, J.B. (2013). Strigolactones and the regulation of pea symbioses in response to nitrate and phosphate deficiency. Mol Plant **6**:76-87. 10.1093/mp/sss115.

Fukaki, H., Tameda, S., Masuda, H., and Tasaka, M. (2002). Lateral root formation is blocked by a gain-of-function mutation in the *SOLITARY-ROOT/IAA14* gene of *Arabidopsis*. The Plant Journal **29**:153-168. https://doi.org/10.1046/j.0960-7412.2001.01201.x.

Fukaki, H., Nakao, Y., Okushima, Y., Theologis, A., and Tasaka, M. (2005). Tissue-specific expression of stabilized *SOLITARY-ROOT/IAA14* alters lateral root development in *Arabidopsis*. The Plant Journal **44**:382-395.

Galinha, C., Hofhuis, H., Luijten, M., Willemsen, V., Blilou, I., Heidstra, R., and Scheres, B. (2007). PLETHORA proteins as dose-dependent master regulators of *Arabidopsis* root development. Nature **449**:1053-1057. 10.1038/nature06206.

Gallois, J.-L., Nora, F.R., Mizukami, Y., and Sablowski, R. (2004). WUSCHEL induces shoot stem cell activity and developmental plasticity in the root meristem. Genes & development **18**:375-380.

Gautrat, P., Mortier, V., Laffont, C., De Keyser, A., Fromentin, J., Frugier, F., and Goormachtig, S. (2019). Unraveling new molecular players involved in the autoregulation of nodulation in *Medicago truncatula*. Journal of Experimental Botany **70**:1407-1417. 10.1093/jxb/ery465.

Gavrin, A., Kulikova, O., Bisseling, T., and Fedorova, E.E. (2017). Interface symbiotic membrane formation in root nodules of *Medicago truncatula:* the role of synaptotagmins *MtSyt1*, *MtSyt2* and *MtSyt3*. Frontiers in Plant Science **8**:201.

Goh, C.-H., Nicotra, A.B., and Mathesius, U. (2018). Genes controlling legume nodule numbers affect phenotypic plasticity responses to nitrogen in the presence and absence of rhizobia. Plant, Cell & Environment **0**10.1111/pce.13498.

Gonzalez-Rizzo, S., Crespi, M., and Frugier, F. (2006). The *Medicago truncatula* CRE1 cytokinin receptor regulates lateral root development and early symbiotic interaction with *Sinorhizobium meliloti*. Plant Cell **18**:2680-2693. 10.1105/tpc.106.043778.

Gourion, B., Berrabah, F., Ratet, P., and Stacey, G. (2015). Rhizobium-legume symbioses: the crucial role of plant immunity. Trends Plant Sci **20**:186-194. 10.1016/j.tplants.2014.11.008.

He, G., Liu, P., Zhao, H., and Sun, J. (2020). The HD-ZIP II Transcription Factors Regulate Plant Architecture through the Auxin Pathway. International Journal of Molecular Sciences **21**:3250.

Heidstra, R., Welch, D., and Scheres, B. (2004). Mosaic analyses using marked activation and deletion clones dissect *Arabidopsis* SCARECROW action in asymmetric cell division. Genes & Development **18**:1964-1969.

Hewitt, E.J. (1966). Sand and water culture methods used in the study of plant nutrition (Commenwealth Agricultural Bureaux).

Hofhuis, H., Laskowski, M., Du, Y., Prasad, K., Grigg, S., Pinon, V., and Scheres, B. (2013). Phyllotaxis and Rhizotaxis in *Arabidopsis* Are Modified by Three PLETHORA Transcription Factors. Current Biology **23**:956-962. 10.1016/j.cub.2013.04.048.

Ivanov, S., Fedorova, E.E., Limpens, E., De Mita, S., Genre, A., Bonfante, P., and Bisseling, T. (2012). Rhizobium-legume symbiosis shares an exocytotic pathway required for arbuscule formation. Proc Natl Acad Sci U S A **109**:8316-8321. 10.1073/pnas.1200407109.

Jan, M., Muhammad, S., Jin, W., Zhong, W., Zhang, S., Lin, Y., Zhou, Y., Liu, J., Liu, H., Munir, R., et al. (2024). Modulating root system architecture: cross-talk between auxin and phytohormones. Front Plant Sci **15**:1343928. 10.3389/fpls.2024.1343928.

Kassaw, T., Jr., W., and Frugoli, J. (2015). Multiple Autoregulation of Nodulation (AON) Signals Identified through Split Root Analysis of *Medicago truncatula sunn* and *rdn1* Mutants. Plants **4**:209.

Khan, M., Xu, H., and Hepworth, S.R. (2014). *BLADE-ON-PETIOLE* genes: Setting boundaries in development and defense. Plant Science **215-216**:157-171. https://doi.org/10.1016/j.plantsci.2013.10.019.

Krusell, L., Madsen, L.H., Sato, S., Aubert, G., Genua, A., Szczyglowski, K., Duc, G., Kaneko, T., Tabata, S., de Bruijn, F., et al. (2002). Shoot control of root development and nodulation is mediated by a receptor-like kinase. Nature **420**:422-426. http://www.nature.com/nature/journal/v420/n6914/suppinfo/nature01207_S1.html.

Krusell, L., Sato, N., Fukuhara, I., Koch, B.E.V., Grossmann, C., Okamoto, S., Oka-Kira, E., Otsubo, Y., Aubert, G., Nakagawa, T., et al. (2011). The *Clavata2* genes of pea and *Lotus japonicus* affect autoregulation of nodulation. Plant Journal **65**:861-871. 10.1111/j.1365-313X.2010.04474.x.

Lagunas, B., Achom, M., Bonyadi-Pour, R., Pardal, A.J., Richmond, B.L., Sergaki, C., Vázquez, S., Schäfer, P., Ott, S., Hammond, J., et al. (2019). Regulation of Resource Partitioning Coordinates Nitrogen and Rhizobia Responses and Autoregulation of Nodulation in *Medicago truncatula*. Mol Plant **12**:833-846. 10.1016/j.molp.2019.03.014.

Laplaze, L., Benkova, E., Casimiro, I., Maes, L., Vanneste, S., Swarup, R., Weijers, D., Calvo, V., Parizot, B., Herrera-Rodriguez, M.B.a., et al. (2007). Cytokinins Act Directly on Lateral Root Founder Cells to Inhibit Root Initiation. The Plant Cell **19**:3889-3900. 10.1105/tpc.107.055863.

Lebedeva, M.A., Sadikova, D.S., Dobychkina, D.A., Zhukov, V.A., and Lutova, L.A. (2022). *CLAVATA3/EMBRYO SURROUNDING REGION* Genes Involved in Symbiotic Nodulation in *Pisum sativum*. Agronomy **12**:2840.

Lee, T., Orvosova, M., Batzenschlager, M., Batista, M.B., Bailey, P.C., Mohd-Radzman, N.A., Gurzadyan, A., Stuer, N., Mysore, K.S., and Wen, J. (2024). Light-sensitive short hypocotyl genes confer symbiotic nodule identity in the legume *Medicago truncatula*. Current Biology **34**:825-840. e827.

Li, D., Kinkema, M., and Gresshoff, P.M. (2009). Autoregulation of nodulation (AON) in *Pisum sativum* (pea) involves signalling events associated with both nodule primordia development and nitrogen fixation. J Plant Physiol **166**:955-967. 10.1016/j.jplph.2009.03.004.

Liao, C.-Y., Smet, W., Brunoud, G., Yoshida, S., Vernoux, T., and Weijers, D. (2015). Reporters for sensitive and quantitative measurement of auxin response. Nature methods **12**:207-210.

Liu, S., Magne, K., Zhou, J., Laude, J., Dalmais, M., Le Signor, C., Bendahmane, A., Thompson, R., Couzigou, J.M., and Ratet, P. (2023). The transcriptional co-regulators NBCL1 and NBCL2 redundantly coordinate aerial organ development and root nodule identity in legumes. J Exp Bot **74**:194-213. 10.1093/jxb/erac389.

Liu, Y.-C., Lei, Y.-W., Liu, W., Weng, L., Lei, M.-J., Hu, X.-H., Dong, Z., Luo, D., and Yang, J. (2018). *LjCOCH* interplays with *LjAPP1* to maintain the nodule development in *Lotus japonicus*. Plant Growth Regulation **85**:267-279. 10.1007/s10725-018-0392-6.

Luo, Z., Liu, H., and Xie, F. (2023). Cellular and molecular basis of symbiotic nodule development. Curr Opin Plant Biol **76**:102478. 10.1016/j.pbi.2023.102478.

Magne, K., George, J., Berbel Tornero, A., Broquet, B., Madueno, F., Andersen, S.U., and Ratet, P. (2018a). *Lotus japonicus NOOT-BOP-COCH-LIKE 1* is essential for nodule, nectary, leaf and flower development. The Plant Journal **94**:880-894.

Magne, K., Couzigou, J.M., Schiessl, K., Liu, S., George, J., Zhukov, V., Sahl, L., Boyer, F., Iantcheva, A., Mysore, K.S., et al. (2018b). *MtNODULE ROOT1* and *MtNODULE ROOT2* Are Essential for Indeterminate Nodule Identity. Plant Physiol **178**:295-316. 10.1104/pp.18.00610.

Mähönen, A.P., Tusscher, K.t., Siligato, R., Smetana, O., Díaz-Triviño, S., Salojärvi, J., Wachsman, G., Prasad, K., Heidstra, R., and Scheres, B. (2014). PLETHORA gradient formation mechanism separates auxin responses. Nature **515**:125-129. 10.1038/nature13663.

McAdam, E.L., Reid, J.B., and Foo, E. (2018). Gibberellins promote nodule organogenesis but inhibit the infection stages of nodulation. Journal of experimental botany **69**:2117-2130.

Miyazawa, H., Oka-Kira, E., Sato, N., Takahashi, H., Wu, G.J., Sato, S., Hayashi, M., Betsuyaku, S., Nakazono, M., Tabata, S., et al. (2010). The receptor-like kinase KLAVIER mediates systemic regulation of nodulation and non-symbiotic shoot development in *Lotus japonicus*. Development **137**:4317-4325. 10.1242/dev.058891.

Moore, W.M., Chan, C., Ishikawa, T., Rennie, E.A., Wipf, H.M.L., Benites, V., Kawai-Yamada, M., Mortimer, J.C., and Scheller, H.V. (2021). Reprogramming sphingolipid glycosylation is required for endosymbiont persistence in *Medicago truncatula*. Current Biology **31**:2374-2385.e2374. 10.1016/j.cub.2021.03.067.

Nadzieja, M., Stougaard, J., and Reid, D. (2019). A Toolkit for High Resolution Imaging of Cell Division and Phytohormone Signaling in Legume Roots and Root Nodules. Front Plant Sci **10**:1000. 10.3389/fpls.2019.01000.

Ng, J.L.P., Hassan, S., Truong, T.T., Hocart, C.H., Laffont, C., Frugier, F., and Mathesius, U. (2015). Flavonoids and auxin transport inhibitors rescue symbiotic nodulation in the *Medicago truncatula* cytokinin perception mutant *cre1*. The Plant Cell **27**:2210-2226.

Nishida, H., Handa, Y., Tanaka, S., Suzaki, T., and Kawaguchi, M. (2016). Expression of the CLE-RS3 gene suppresses root nodulation in *Lotus japonicus*. Journal of Plant Research **129**:909-919. 10.1007/s10265-016-0842-z.

Oka-Kira, E., Tateno, K., Miura, K.i., Haga, T., Hayashi, M., Harada, K., Sato, S., Tabata, S., Shikazono, N., and Tanaka, A. (2005). *klavier* (*klv*), a novel hypernodulation mutant of *Lotus japonicus* affected in vascular tissue organization and floral induction. The Plant Journal **44**:505-515.

Pimentel, H., Bray, N.L., Puente, S., Melsted, P., and Pachter, L. (2017). Differential analysis of RNA-seq incorporating quantification uncertainty. Nature Methods **14**:687-690. 10.1038/nmeth.4324.

Qi, B., and Zheng, H. (2013). Modulation of root-skewing responses by KNAT1 in *Arabidopsis thaliana*. The Plant Journal **76**:380-392. https://doi.org/10.1111/tpj.12295.

Racolta, A., Nodine, M.D., Davies, K., Lee, C., Rowe, S., Velazco, Y., Wellington, R., and Tax, F.E. (2018). A Common Pathway of Root Growth Control and Response to CLE Peptides Through Two Receptor Kinases in Arabidopsis. Genetics **208**:687-704. 10.1534/genetics.117.300148.

Radhakrishnan, G.V., Keller, J., Rich, M.K., Vernié, T., Mbadinga, D.L.M., Vigneron, N., Cottret, L., San Clemente, H., Libourel, C., and Cheema, J. (2020). An ancestral signalling pathway is conserved in intracellular symbioses-forming plant lineages. Nature Plants:1-10.

Ramon, U., Weiss, D., and Illouz-Eliaz, N. (2021). Underground gibberellin activity. The New Phytologist **229**:1196-1200.

Reid, D., Nadzieja, M., Novák, O., Heckmann, A.B., Sandal, N., and Stougaard, J. (2017). Cytokinin biosynthesis promotes cortical cell responses during nodule development. Plant Physiology **175**:361-375.

Riefler, M., Novak, O., Strnad, M., and Schmülling, T. (2006). *Arabidopsis* cytokinin receptor mutants reveal functions in shoot growth, leaf senescence, seed size, germination, root development, and cytokinin metabolism. The Plant Cell **18**:40-54.

Rodriguez, R.E., Ercoli, M.F., Debernardi, J.M., Breakfield, N.W., Mecchia, M.A., Sabatini, M., Cools, T., De Veylder, L., Benfey, P.N., and Palatnik, J.F. (2015). MicroRNA miR396 Regulates the Switch

between Stem Cells and Transit-Amplifying Cells in *Arabidopsis* Roots. The Plant Cell **27**:3354-3366. 10.1105/tpc.15.00452.

Roppolo, D., De Rybel, B., Tendon, V.D., Pfister, A., Alassimone, J., Vermeer, J.E., Yamazaki, M., Stierhof, Y.-D., Beeckman, T., and Geldner, N. (2011). A novel protein family mediates Casparian strip formation in the endodermis. Nature **473**:380-383.

Roy, S., and Muller, L.M. (2022). A rulebook for peptide control of legume-microbe endosymbioses. Trends Plant Sci **27**:870-889. 10.1016/j.tplants.2022.02.002.

Roy, S., Liu, W., Nandety, R.S., Crook, A., Mysore, K.S., Pislariu, C.I., Frugoli, J., Dickstein, R., and Udvardi, M.K. (2020). Celebrating 20 Years of Genetic Discoveries in Legume Nodulation and Symbiotic Nitrogen Fixation. The Plant Cell **32**:15. 10.1105/tpc.19.00279.

Sagan, M., and Duc, G. (1996). *Sym28* and *Sym29*, two new genes involved in regulation of nodulation in pea (*Pisum sativum* L.). Symbiosis.

Santuari, L., Sanchez-Perez, G.F., Luijten, M., Rutjens, B., Terpstra, I., Berke, L., Gorte, M., Prasad, K., Bao, D., Timmermans-Hereijgers, J.L.P.M., et al. (2016). The *PLETHORA* Gene Regulatory Network Guides Growth and Cell Differentiation in *Arabidopsis* Roots. The Plant Cell **28**:2937-2951. 10.1105/tpc.16.00656.

Schiessl, K., Lilley, J.L.S., Lee, T., Tamvakis, I., Kohlen, W., Bailey, P.C., Thomas, A., Luptak, J., Ramakrishnan, K., Carpenter, M.D., et al. (2019). *NODULE INCEPTION* Recruits the Lateral Root Developmental Program for Symbiotic Nodule Organogenesis in *Medicago truncatula*. Curr Biol **29**:3657-3668 e3655. 10.1016/j.cub.2019.09.005.

Schnabel, E.L., Chavan, S.A., Gao, Y., Poehlman, W.L., Feltus, F.A., and Frugoli, J.A. (2023). A *Medicago truncatula* autoregulation of nodulation mutant transcriptome analysis reveals disruption of the SUNN pathway causes constitutive expression changes in some genes, but overall response to rhizobia resembles wild-type, including induction of *TML1* and *TML2*. Current Issues in Molecular Biology **45**:4612-4631.

Schnabel, E.L., Kassaw, T.K., Smith, L.S., Marsh, J.F., Oldroyd, G.E., Long, S.R., and Frugoli, J.A. (2011). The *ROOT DETERMINED NODULATION1* gene regulates nodule number in roots of *Medicago truncatula* and defines a highly conserved, uncharacterized plant gene family. Plant Physiology **157**:328-340.

Scott, T., Correa-Lozano, A., and Foo, E. (2024). Upstairs, Downstairs - conserved and divergent CLAVATA signalling in shoot meristem development and root symbioses. Ann Bot 10.1093/aob/mcae192.

Sevin-Pujol, A., Sicard, M., Rosenberg, C., Auriac, M.C., Lepage, A., Niebel, A., Gough, C., and Bensmihen, S. (2017). Development of a GAL4-VP16/UAS trans-activation system for tissue specific expression in *Medicago truncatula*. PLoS One **12**:e0188923. 10.1371/journal.pone.0188923.

Shen, D., Kulikova, O., Guhl, K., Franssen, H., Kohlen, W., Bisseling, T., and Geurts, R. (2019). The *Medicago truncatula* nodule identity gene *MtNOOT1* is required for coordinated apical-basal development of the root. BMC Plant Biol **19**:571. 10.1186/s12870-019-2194-z.

Shen, D., Xiao, T.T., van Velzen, R., Kulikova, O., Gong, X., Geurts, R., Pawlowski, K., and Bisseling, T. (2020a). A homeotic mutation changes legume nodule ontogeny into actinorhizal-type ontogeny. The Plant Cell **32**:1868-1885.

Shen, D., Xiao, T.T., van Velzen, R., Kulikova, O., Gong, X., Geurts, R., Pawlowski, K., and Bisseling, T. (2020b). A Homeotic Mutation Changes Legume Nodule Ontogeny into Actinorhizal-Type Ontogeny. Plant Cell **32**:1868-1885. 10.1105/tpc.19.00739.

Shrestha, A., Zhong, S., Therrien, J., Huebert, T., Sato, S., Mun, T., Andersen, S.U., Stougaard, J., Lepage, A., and Niebel, A. (2021). *Lotus japonicus Nuclear Factor YA1*, a nodule emergence stage-specific regulator of auxin signalling. New Phytologist **229**:1535-1552.

Sin, W.-C., Liu, J., Zhong, J.Y., Lam, H.-M., and Lim, B.L. (2024). Comparative proteomics analysis of root and nodule mitochondria of soybean. Plant, Cell & Environment **n/a**https://doi.org/10.1111/pce.15026.

Soyano, T., Shimoda, Y., Kawaguchi, M., and Hayashi, M. (2019). A shared gene drives lateral root development and root nodule symbiosis pathways in *Lotus*. Science **366**:1021-1023. 10.1126/science.aax2153.

Suzaki, T., Yano, K., Ito, M., Umehara, Y., Suganuma, N., and Kawaguchi, M. (2012). Positive and negative regulation of cortical cell division during root nodule development in *Lotus japonicus* is accompanied by auxin response. Development **139**:3997-4006.

Tan, S., Sanchez, M., Laffont, C., Boivin, S., Le Signor, C., Thompson, R., Frugier, F., and Brault, M. (2020). A Cytokinin Signaling Type-B Response Regulator Transcription Factor Acting in Early Nodulation. Plant Physiol **183**:1319-1330. 10.1104/pp.19.01383.

Tong, C., Zhang, Y., and Shi, F. (2023). Genome-wide identification and analysis of the *NLR* gene family in *Medicago ruthenica*. Frontiers in Genetics **13**:1088763.

Triozzi, P.M., Irving, T.B., Schmidt, H.W., Keyser, Z.P., Chakraborty, S., Balmant, K., Pereira, W.J., Dervinis, C., Mysore, K.S., and Wen, J. (2022). Spatiotemporal cytokinin response imaging and ISOPENTENYLTRANSFERASE 3 function in *Medicago* nodule development. Plant Physiology **188**:560-575.

Truernit, E., and Haseloff, J. (2007). A Role for KNAT Class II Genes in Root Development. Plant Signal Behav **2**:10-12. 10.4161/psb.2.1.3604.

Tu, T., Gao, Z., Li, L., Chen, J., Ye, K., Xu, T., Mai, S., Han, Q., Chen, C., Wu, S., et al. (2024). Soybean symbiotic-nodule zonation and cell differentiation are defined by NIN2 signaling and GH3-dependent auxin homeostasis. Dev Cell 10.1016/j.devcel.2024.07.001.

Ubeda-Tomás, S., Federici, F., Casimiro, I., Beemster, G.T., Bhalerao, R., Swarup, R., Doerner, P., Haseloff, J., and Bennett, M.J. (2009). Gibberellin signaling in the endodermis controls *Arabidopsis* root meristem size. Current Biology **19**:1194-1199.

Van de Velde, W., Zehirov, G., Szatmari, A., Debreczeny, M., Ishihara, H., Kevei, Z., Farkas, A., Mikulass, K., Nagy, A., Tiricz, H., et al. (2010). Plant peptides govern terminal differentiation of bacteria in symbiosis. Science **327**:1122-1126. 10.1126/science.1184057.

Velandia, K., Reid, J.B., and Foo, E. (2022). Right time, right place: The dynamic role of hormones in rhizobial infection and nodulation of legumes. Plant Commun:100327. 10.1016/j.xplc.2022.100327.

Velandia, K., Correa-Lozano, A., McGuiness, P.M., Reid, J.B., and Foo, E. (2024). Cell-layer specific roles for gibberellins in nodulation and root development. New Phytologist **242**:626-640.

Wang, C., Reid, J.B., and Foo, E. (2020). The role of CLV1, CLV2 and HPAT homologues in the nitrogen-regulation of root development. Physiol Plant 10.1111/ppl.13200.

Wang, D., Griffitts, J., Starker, C., Fedorova, E., Limpens, E., Ivanov, S., Bisseling, T., and Long, S. (2010). A nodule-specific protein secretory pathway required for nitrogen-fixing symbiosis. Science **327**:1126-1129. 10.1126/science.1184096.

Wang, Y., Li, K., Chen, L., Zou, Y., Liu, H., Tian, Y., Li, D., Wang, R., Zhao, F., Ferguson, B.J., et al. (2015). MicroRNA167-Directed Regulation of the Auxin Response Factors GmARF8a and GmARF8b Is Required for Soybean Nodulation and Lateral Root Development Plant Physiology **168**:984-999. 10.1104/pp.15.00265.

Wopereis, J., Pajuelo, E., Dazzo, F.B., Jiang, Q., Gresshoff, P.M., De Bruijn, F.J., Stougaard, J., and Szczyglowski, K. (2000). Short root mutant of *Lotus japonicus* with a dramatically altered symbiotic phenotype. The Plant Journal **23**:97-114.

Xiao, T.T., Müller, S., Shen, D., Liu, J., Adema, K., van Seters, A., Franssen, H., Bisseling, T., Kulikova, O., and Kohlen, W. (2025). Nodule organogenesis in *Medicago truncatula* requires local stage-specific auxin biosynthesis and transport. Plant Physiology **197**10.1093/plphys/kiaf133.

Yan, W., Wang, R., Zhang, Y., Zhang, X., and Wang, Q. (2024). A *Medicago truncatula* HD-ZIP gene MtHB2 is involved in modulation of root development by regulating auxin response. Front Plant Sci **15**:1466431. 10.3389/fpls.2024.1466431.

Yang, S., Tang, F., Gao, M., Krishnan, H.B., and Zhu, H. (2010). R gene-controlled host specificity in the legume-rhizobia symbiosis. Proc Natl Acad Sci U S A **107**:18735-18740. 10.1073/pnas.1011957107.

Ye, L., Wang, X., Lyu, M., Siligato, R., Eswaran, G., Vainio, L., Blomster, T., Zhang, J., and Mähönen, A.P. (2021). Cytokinins initiate secondary growth in the *Arabidopsis* root through a set of *LBD* genes. Current Biology **31**:3365-3373.e3367. https://doi.org/10.1016/j.cub.2021.05.036.

Yoro, E., Suzaki, T., and Kawaguchi, M. (2019). CLE-HAR1 Systemic Signaling and NIN-Mediated Local Signaling Suppress the Increased Rhizobial Infection in the daphne Mutant of *Lotus japonicus*. Molecular Plant-Microbe Interactions:MPMI-08-19-0223-R. 10.1094/MPMI-08-19-0223-R.

Zhang, M., Su, H., Gresshoff, P.M., and Ferguson, B.J. (2021). Shoot-derived miR2111 controls legume root and nodule development. Plant Cell Environ **44**:1627-1641. 10.1111/pce.13992.

Zuo, Z., Roux, M.E., Chevalier, J.R., Dagdas, Y.F., Yamashino, T., Højgaard, S.D., Knight, E., Østergaard, L., Rodriguez, E., and Petersen, M. (2023). The mRNA decapping machinery targets LBD3/ASL9 to mediate apical hook and lateral root development. Life Sci Alliance **6**10.26508/lsa.202302090.

Zürcher, E., Tavor-Deslex, D., Lituiev, D., Enkerli, K., Tarr, P.T., and Müller, B. (2013). A robust and sensitive synthetic sensor to monitor the transcriptional output of the cytokinin signaling network in planta. Plant physiology **161**:1066-1075.